UC Riverside
UC Riverside Previously Published Works

Title

CCR5 Knockout Prevents Neuronal Injury and Behavioral Impairment Induced in a Transgenic Mouse Model by a CXCR4-Using HIV-1 Glycoprotein 120

Permalink

https://escholarship.org/uc/item/5pb738q6

Journal

The Journal of Immunology, 193(4)

ISSN

0022-1767

Authors

Maung, Ricky
Hoefer, Melanie M
Sanchez, Ana B
et al.

Publication Date

2014-08-15

DOI

10.4049/jimmunol.1302915

Peer reviewed

CCR5 Knockout Prevents Neuronal Injury and Behavioral Impairment Induced in a Transgenic Mouse Model by a CXCR4-using HIV-1 Glycoprotein 120[1]

Ricky Maung[*], **Melanie M. Hoefer**[*], **Ana B. Sanchez**[*], **Natalia E. Sejbuk**[*], **Kathryn E. Medders**[*,†], **Maya K. Desai**[†], **Irene C. Catalan**[*], **Cari C. Dowling**[*], **Cyrus M. de Rozieres**[*], **Gwenn A. Garden**[‡], **Rossella Russo**[†,§], **Amanda J. Roberts**[¶], **Roy Williams**[||], and **Marcus Kaul**[*,†,#]

[*]Infectious and Inflammatory Disease Center, Sanford-Burnham Medical Research Institute, 10901 North Torrey Pines Road, La Jolla, CA 92037, USA

[†]Neuroscience, Aging and Stem Cell Research Center, Sanford-Burnham Medical Research Institute, 10901 North Torrey Pines Road, La Jolla, CA 92037, USA

[||]Bioinformatics Shared Resource, Sanford-Burnham Medical Research Institute, 10901 North Torrey Pines Road, La Jolla, CA 92037, USA

[‡]Department of Neurology, University of Washington, 1959 NE Pacific St, HSB RR-637, Seattle, WA 98195

[§]Department of Pharmacobiology, University of Calabria, 87036 Arcavacata di Rende, Italy

[¶]Molecular & Cellular Neurosciences Department, The Scripps Research Institute, 10550 N. Torrey Pines Rd, MB18, La Jolla, CA 92037, USA

[#]Department of Psychiatry, University of California, San Diego, 9500 Gilman Dr., La Jolla, CA 92093, USA

Abstract

The innate immune system has been implicated in several neurodegenerative diseases, including human immunodeficiency virus (HIV)-1 associated dementia. Here we show that genetic ablation of CCR5 prevents microglial activation and neuronal damage in a transgenic model of HIV-associated brain injury induced by a CXCR4-utilizing viral envelope gp120. The CCR5 knockout (KO) also rescues spatial learning and memory in gp120-transgenic (tg) mice. However, the CCR5KO does not abrogate astrocytosis, indicating it can occur independently from neuronal injury and behavioral impairment. To further characterize the neuroprotective effect of CCR5-deficiency we performed a genome –wide gene expression analysis of brains from HIVgp120tg

Corresponding author: Marcus Kaul, Infectious and Inflammatory Disease Center, Sanford-Burnham Medical Research Institute, 10901 North Torrey Pines Road, La Jolla, CA 92037, USA (mkaul@sanfordburnham.org) Tel. 001 858 795-5215, Fax 001 858 795-5225.

Disclosures
The authors have no financial conflicts of interest.

mice expressing or lacking CCR5 and non-transgenic controls. Comparison with a human brain microarray study reveals that brains of HIVgp120tg mice and HIV patients with neurocognitive impairment share numerous differentially regulated genes. Furthermore, brains of CCR5 wild-type (WT) and CCR5KO gp120tg mice express markers of an innate immune response. One of the most significantly up-regulated factors is the acute phase protein lipocalin-2 (LCN2). Using cerebrocortical cell cultures, we find that LCN2 is neurotoxic in a CCR5-dependent fashion while inhibition of CCR5 alone is not sufficient to abrogate neurotoxicity of a CXCR4-utilizing gp120. However, the combination of pharmacological CCR5 blockade and LCN2 protects neurons from toxicity of a CXCR4-utilizing gp120 thus recapitulating the finding in CCR5-deficient gp120tg mouse brain. Altogether, our study provides evidence for an indirect pathological role of CCR5 and a novel protective effect of LCN2 in combination with inhibition of CCR5 in HIV-associated brain injury.

Introduction

The chemokine receptors CCR5 and CXCR4 are co-receptors besides CD4 for HIV infection (1). CCR5 deficiency due to a congenital deletion mutation, named CCR5 32, leads to absence of this receptor from the cell surface and confers protection against infection with CCR5-prefering HIV-1 (2). Experimental knock-down of CCR5 in human macrophages also can prevent infection of the cells with CCR5-prefering virus (3). CCR5 deficiency is *per se* not associated with a pathological phenotype in human beings (2) or in mice (4,5). However, CCR5 knockout (KO) and wild-type (WT) animals differ in their responses to infections, including the migration of peripheral monocytes and macrophages into the central nervous system (CNS) (4,5). Moreover, CCR5-deficient macrophages show upon stimulation reduced cytokine production of GM-CSF, IL-1β and IL-6 compared to their WT counterparts (4). Independently of a function in HIV entry, CCR5 and its endogenous ligands CCL3, CCL4 and CCL5 can delay progression to AIDS (6,7). However, once HIV infection is established, dual tropic and CXCR4-preferring viruses often evolve, and usually herald progression to AIDS and HIV-associated dementia (1,8–11).

Transgenic (tg) mice expressing a soluble viral envelope gp120 of HIV-1 LAV in the brain have previously been described (12). The CXCR4-using HIV-1 LAV isolate infects lymphocytes and macrophages (13). We recently showed in mixed neuronal-glial cerebrocortical cell cultures from mice genetically deficient in CCR5 or CXCR4, or both co-receptors, that the specificity of HIV gp120 co-receptor usage in the mouse model resembled that in human cells (14). The soluble transgenic gp120 is expressed in astrocytes under the control of the promoter for glial fibrillary acidic protein (GFAP) and can be detected by immunoblotting in brain extracts (15). HIVgp120tg mice manifest several neuropathological features observed in AIDS brains, such as decreased synaptic and dendritic density, increased numbers of activated microglia and astrocytosis (12,16–19). HIVgp120tg mice also develop behavioral impairment, such as reduced escape latency, swimming velocity, and spatial retention before 12 months of age (20,21).

Here we show that genetic ablation of CCR5 prevents neuronal injury and microglial activation in HIVgp120tg mice even though the transgenic gp120 utilizes CXCR4. CCR5-

deficiency also protects gp120tg mice against impairment of spatial learning and memory. However, CCR5-ablation fails to abrogate astrocytosis. Genome-wide gene expression analysis shows that gp120tg brains up-regulate among other factors of the innate immune system the acute phase protein lipocalin (LCN) 2, which promotes activation while also priming the demise of microglia (22,23). We find that LCN2 is itself neurotoxic in a CCR5-dependent fashion. Moreover, we observe that blockade of CCR5 signaling and LCN2 cooperate to diminish microglial cell numbers and to prevent neurotoxicity of a CXCR4-utilizing gp120, thus recapitulating the findings in CCR5-deficient gp120tg mice.

Materials and Methods

Animals

Two founder lines of HIVgp120tg mice were kindly provided by Dr. Lennart Mucke (Gladstone Institute of Neurological Disease, University of California, San Francisco, CA) (12). CCR5 knockout mice (CCR5KO, B6.129P2-*Ccr5*^{tm1Kuz}/J) were purchased from The Jackson Laboratory. CCR5KO and HIV gp120tg mice were crossbred and F2 animals heterozygous for CCR5 and HIV gp120 were used to generate colonies comprising all necessary genotypes. Genotyping was performed according to protocols published in the literature (12) and by The Jackson Laboratory. All experimental procedures and protocols involving animals were in accordance with NIH guidelines and approved by the Institutional Animal Care and Use Committees of the Sanford-Burnham Medical Research Institute and The Scripps Research Institute.

Behavioral testing

WT, gp120, CCR5KO and CCR5KO x gp120 mice were between eight and nine months of age at the beginning of testing that occurred over a period of five weeks.

Light/dark transfer test—The light/dark transfer procedure has been used to assess anxiety-like behavior in mice (24) and was performed as previously described (25). In brief, the apparatus is a rectangular box made of Plexiglas divided by a partition into two environments. One compartment is dark and the other compartment is highly illuminated by a light source located above it. The compartments are connected by an opening located at floor level in the center of the partition. The time spent in the light compartment is used as a predictor of anxiety-like behavior. Mice were placed in the dark compartment to start the 5 min test.

Locomotor activity test—Activity levels were measured in polycarbonate cages placed into frames mounted with two levels of photocell beams at 2 and 7 cm above the bottom of the cage (San Diego Instruments, San Diego, CA) as recently published (26). These two sets of beams allowed for the recording of both horizontal (locomotion) and vertical (rearing) behavior. A thin layer of bedding material was applied to the bottom of the cage. Mice were tested for 2 h.

Barnes maze test—The Barnes maze test assesses spatial learning and memory (27,28). In addition, the test reveals the strategies used by the animals to perform the task. The test

was performed as previously published with minor modifications (29). The Barnes maze used was an opaque Plexiglas disc 75 cm in diameter elevated 58 cm above the floor by a tripod. Twenty holes, 5 cm in diameter, were located 5 cm from the perimeter, and a black Plexiglas escape box was placed under one of the holes. Distinct spatial cues were located all around the maze and were kept constant throughout the study. Mice were tested once a day for 9 days for the acquisition portion of the study. For the Probe Test, the 10th test, the escape tunnel was removed and the mouse was allowed to freely explore the maze for 3 min. The time spent in each quadrant was determined and the percent time spent in the target quadrant was compared with the average percent time in the other three quadrants. Each session was videotaped and scored by an experimenter blind to the genotype of the mouse. Measures recorded included the latency to escape, the number of errors made per session and the strategy employed by the mouse to locate the escape tunnel. Search strategies were determined by examining each mouse's daily session and classifying it into one of three operationally defined categories: 1) Random search strategy - localized hole searches separated by crossings through the center of the maze, 2) Serial search strategy - systematic hole searches (every hole or every other hole) in a clockwise or counterclockwise direction, or 3) Spatial search strategy - reaching the escape tunnel with both error and distance (number of holes between the first hole visited and the escape tunnel) scores of less than or equal to 3.

Immunofluorescence and deconvolution microscopy

For neuropathological assessment mice were deeply anesthetized with Isofluran and immediately transcardially perfused with 0.9 % saline. Brains were quickly removed and fixed with 4 % paraformaldehyde in phosphate-buffered saline (PBS, pH 7.4) for 48 hours at 4°C. All experimental animals were coded before the process of analysis. For histopathological analysis, 30 μm thick sagittal sections were permeabilized with 1 % Triton X-100 (freshly prepared) in PBS for 30 min. Non-specific binding sites were blocked with 10 % heat-inactivated goat serum in PBS containing 0.05 % Tween 20 (PBS-T) for 1.5 h. Floating sections were immunostained with an anti-MAP-2 mAb (1 : 500; Sigma) and a polyclonal rabbit anti-synaptophysin (1 : 500; Dako) as neuronal markers, or Iba1 (1 : 125; Wako) and GFAP (1 : 500; Dako) as microglial and astrocytic markers, respectively. Rhodamine-conjugated goat anti-mouse (1 : 200; Jackson ImmunoResearch) and Alexa Fluor 488-labelled goat anti-rabbit (1 : 200; Molecular Probes/Life Technologies) in 5 % goat serum in PBS-T were used as secondary antibodies. Nuclear DNA was labeled with H33342 (12 μM in PBS).

Observers blinded to genotype analyzed neuronal damage and gliosis in neocortex and hippocampus using an inverted Axiovert 100M fluorescence microscope (Zeiss) fitted with a computer controlled 3D stage, the appropriate filter sets and a CCD camera. We analyzed per animal and marker at least three sagittal sections spaced at 300 μm distance from each other medial to lateral. For each section we recorded five fields (cerebral cortex) and three fields (hippocampus), using 40 x image stacks at 0.5 μm steps along the Z axis. Deconvolution microscopy and fluorescence and volumetric quantitation was performed with the Slidebook software package (Intelligent Imaging Innovations, Denver, CO) (12,14,30). After deconvolution with a constrained iterative algorithm the percentage of

neuropil occupied by MAP-2^{+} dendrites and Syp[+] presynaptic terminals was determined by threshold segmentation and compared between the different genotype groups. GFAP fluorescence was quantified in 10 x images using masks for areas of interest. For quantification of Iba1^{+} microglia, we counted cell bodies on the lateral side of three sagittal sections per animal in the area of interest in cerebral cortex and hippocampus.

For analysis of microglial TNFα additional brain sections were incubated with mouse anti TNFα monoclonal antibody (1 : 100; Santa Cruz) in combination with the rabbit anti-Iba1 antibody. A donkey anti-rabbit IgG labeled with Alexa Fluor 647 (1 : 400; Invitrogen) and Rhodamine Red-conjugated goat anti-mouse IgG served as secondary antibodies. DNA was labeled with H33342. Staining with irrelevant IgG of the same isotype and omission of primary antibody served as controls. Threshold segmentation for Iba1 fluorescence was employed to define the areas occupied by microglial cell bodies. Specific fluorescence intensities were estimated for TNFα within microglial cells using the Slidebook software package.

LCN2 was detected using a rat anti mouse LCN2 IgG (1 : 500; R&D Systems) and a secondary chicken anti rat antibody labeled with Alexa 488 (1 : 400; Invitrogen). Staining for LCN2 was combined with one of the above mentioned antibodies for Iba1, GFAP or MAP-2 and the matching anti rabbit or anti mouse secondary antibodies conjugated to Rhodamine Red (Jackson ImmunoResearch).

Microarray

For analysis of whole-genome gene expression mice were placed under deep general anesthesia with Isofluran and immediately transcardially perfused with 0.9 % saline. Brains were quickly removed and snap frozen in liquid nitrogen. All RNA was purified in our laboratory using the QIAGEN RNeasy Lipid Tissue Midi Kit (QIAGEN, Valencia, CA) according to the manufacturer's instructions. Sample amplification, labeling and hybridization on Illumina mouse WG6 v2 Sentrix BeadChips were performed for all arrays in this study according to the manufacturer's instructions (Illumina) and primary hybridization data were collected using an Illumina BeadStation (Sanford Burnham Institute Microarray Core). For line 1 and 2 sample array data was each divided up into 20 groups of replicates by genotype and age; numbers indicate months of age, numbers in brackets show biological replicate samples in the group (n): Line 1: months 1.5/3/6/12/20, *WT*: (6/6/4/6/6); *gp120*: (7/6/5/6/5); *CCR5KO*: (3/5/6/6/5); *CCR5KO x gp120*: (5/3/4/6/5). Line 2: months 1.5/3/6/12/16, *WT*: (7/6/5/6/3); *gp120*: (6/7/7/8/6); *CCR5KO*: (7/6/4/8/3); *CCR5KO x gp120*: (6/7/7/8/4). The data were treated independently as line 1 (104 arrays) and line 2 (121 arrays). Initially, the primary Illumina mouse WG-6 array data was quality controlled by using the Illumina Beadstudio detection *P*-value set to < 0.05 as a cutoff for continued inclusion in the analysis. After filtering, 37,349 and 34,749 probes were retained for the line 1 and line 2 experiments, respectively. The data were then quantiles normalized, log2 transformed, and the limma function *removeBatchEffects* was used to alleviate any chip dependent fluctuations. GeneSpring GX12 expression analysis software was employed to carry out 2-way ANOVAs looking at the variation in CNS gene expression as a function of mouse age and HIV gp120 genotype separately in CCR5WT and CCR5KO backgrounds

and for both mouse lines 1 and 2. The samples were paired by age for each series. The *P*-value cutoff 0.05 was used to determine significance for differential expression between the conditions. This was followed by intersecting the significant results from the two lines to obtain those genes which were *commonly* differentially expressed (*core common set of genes*). Hypergeometric tests found the overlaps between line1 and 2 for genotype to be highly significant ($P < 1 \times 10^{-308}$). The microarray data generated in this study have been deposited in the GEO database under accession number GSE47029. http://www.ncbi.nlm.nih.gov/geo/query/acc.cgi?token=jhgxnkcscagistw&acc=GSE47029

Bioinformatics

For comparison of differentially expressed genes in brains of HIV patients (31) with the *core common set of genes* for CCR5KO x HIV gp120tg mouse lines 1 and 2, the published human gene probe lists were matched with corresponding mouse probes using the BioMart Gene ID Converter tool (www.ensembl.org) and the comparison were performed using GeneSpring GX12.

The lists of the *core common set of genes* for CCR5KO x HIV gp120tg mouse lines 1 and 2 were exported and uploaded to the commercially available bioinformatic tools of Ingenuity Pathway Analysis (IPA, Ingenuity® Systems, www.ingenuity.com). Using these tools the lists were evaluated for enrichment in biologically related genes and involvement in biological canonical pathways. Canonical pathway analyses were generated through the use of IPA and heatmaps using the tool HierarchicalClusteringImage with the default color map of GenePattern 3.5.0 software (Broad Institute).

Quantitative reverse transcription polymerase chain reaction (qRT-PCR)

RNA was isolated from frozen mouse brain tissue as described above for microarray experiments. Reverse transcription (RT) was performed using SuperScript II reverse transcriptase (Invitrogen, Life Technologies Corp. Carlsbad, CA. USA) following the manufacturer's instructions with some modifications. Briefly, 500 ng of RNA purified from mouse brain tissue was used to generate cDNA and preparations were aliquoted, and conserved at $-20\ ^\circ$C until use. Real time PCR was performed using Power PCR SYBR Green mastermix (Applied Biosystems, Life Technologies Corp., Carlsbad, CA, USA). The amplification reactions were carried out in a total volume of 20 μl containing 2 μl of RT, 10 μl of Power PCR SYBR Green mastermix (including HotStart DNA polymerase, reaction buffer, dNTP mix and SYBR Green dye), 0.5 μM of specific primers (Table I) and 8 μl of PCR grade water. PCR amplification was performed on an Mx3000P system (Stratagene, Agilent Technologies) using universal thermal conditions: 10 min at 95 °C and 40 cycles of 15 s at 95 °C and 1 min at 60 °C. A denaturation step was added at the end of the amplification reaction for Tm analysis. The results obtained were analyzed using SDS v1.2 software (Stratagene, Agilent Technologies). RNA samples corresponding to three to six biological replicates were analyzed. The signal for GAPDH was used to normalize the data. The relative amount of mRNA of every gene versus the internal controls (GAPDH) was calculated following the $2^{-\ \triangle Ct}$ method. Murine gene sequences were retrieved from the GenBank database (www.ncbi.nlm.nih.org) for primer design. Primers were designed using 3 different sources: i) PrimerBank (http://pga.mgh.harvard.edu/primerbank/), ii) Primer3

(http://frodo.wi.mit.edu/) and iii) Primer Express software sequences from the 7300 Real-Time PCR System (Applied Biosystems, Foster, CA, USA).

Flow cytometry

Brain mononuclear cells were enriched and analyzed following a published protocol (32). Cell suspensions from five mice were pooled and then fractionated on a discontinuous Percoll gradient. For comparison of CD45 high and CD45 low populations, spleens were also collected, minced and stained with the same antibodies as the brain mononuclear cells. After blocking Fc receptors with anti-CD16/32, cells were stained for extracellular markers with antibodies to CD11b conjugated to PerCP-Cy5.5 (clone M1/70) and CD45 conjugated to APC (clone 30-F11), or with isotype controls for the respective antibody (all eBioscience, San Diego, CA, USA). After washing, cells were fixed for 20 min in 2 % PFA/PBS on ice. Data were acquired on a FACSCanto flow cytometer (BD Biosciences, San Jose, CA, USA) and analyzed using FlowJo (Tree Star Inc., Ashland, OR, USA). Using the forward/side scatter (FSC/SSC) plot, gates were set on live cells, and these were further gated on singlets in the forward scatter area/height (FSC-A/FSC-H) plot to eliminate doublets or aggregates. Next, singlets were analyzed by CD11b-PerCP-Cy5.5 and CD45-APC expression. To quantify CD45low and CD45high expressing cells, splenocytes were analyzed in the same way and gates were set according to the CD45high expressing cells. Each plot represents the analysis of $4 - 10 \times 10^4$ events.

In vitro cell culture experiments

Cerebrocortical cell cultures containing neurons, astrocytes and microglia were generated from E14.5 embryos of mouse line 2 as described previously with minor modifications (14,33). Dissociated cerebrocortical cells were plated at 7×10^4 cells per well in 96 well flat bottom plates for imaging (BD Falcon, Franklin Lake, NJ, USA). Generally, the cells were used for experiments at day in vitro 17. In brief, we exposed cerebrocortical cell cultures to the CXCR4-using gp120 of HIV-1$_{IIIB}$ (1 nM) in the presence or absence of recombinant murine LCN2 (4 nM; R&D Systems) or the CCR5 inhibitor Maraviroc (MVC; 5 nM) for three days. After fixation and labeling of microglia, neurons and nuclear DNA with Tomato lectin, anti MAP-2 antibody and Hoechst 33342, respectively, the cerebrocortical cultures were analyzed by fluorescence microscopy and cell counting (5 fields each per 9 – 10 replicates per condition) as previously described (14,33). Recombinant gp120 of HIV-1$_{IIIB}$ and MVC were obtained from the NIH AIDS Research and Reference Reagent Program.

For analysis of microglial TNFα and ARG1, exposed, fixed and permeablized cerebrocortical cells cultures on glass coverslips (14,33) were incubated with mouse anti TNFα (1 : 100; Santa Cruz) or rabbit anti ARG1 IgG (1 : 200; Santa Cruz). Goat anti-mouse and donkey anti-rabbit IgG conjugated to Alexa Fluor 488 (1 : 400; Invitrogen) served as respective secondary antibodies. Fluorescence staining with irrelevant IgG of the same isotype served as controls. The immunostaining was combined with Texas Red-conjugated Tomato lectin (1 : 200; Vector) and H33342 for labeling of microglia and nuclear DNA, respectively. Quantitative microscopic analysis was performed as described above for mouse brain sections using the Slidebook software package. Threshold segmentation for Tomato

lection was used to define the areas occupied by microglial cell bodies. Specific fluorescence intensities were estimated for TNFα and ARG1 within microglial cells.

ELISA

Protein extracts from brains were prepared using a modification of an earlier described protocol for cell lysis (33). In brief, 250 mg brain tissue was submerged in 2 ml of ice-cold cell lysis buffer and carefully homogenized with a bounce homogenizer. After sonication in ice water the extract was centrifuged at $13,000 \times g$ for 10 min at 4°C. The clear lysate supernatant was aliquoted for storage at $-80°$ C. Lysates were standardized for protein content/brain using a BCA protein assay kit (Pierce, Thermo Fisher, Rockford, IL) before analysis of proteins with specific ELISAs (R&D Systems, Minneapolis, MN) according to the supplier's instructions.

Statistical analysis

Data sets from quantification of immunoreactive neuropil, ELISA, cell counts, FACS, qRT-PCR and indicated components of the behavioral test battery were subjected to analysis of variance (ANOVA) followed by Fisher's PLSD post hoc test using the StatView software package (version 5.0.1, SAS Institute, Cary, NC). Use of spatial strategy was compared using a Chi square test. Significance level for all analyses was $P = 0.05$.

Results

CCR5KO abrogates neuronal injury associated with expression of CXCR4-using HIV gp120

In order to assess *in vivo* whether CCR5 exerted effects beyond its function as gp120 co-receptor and as such influenced brain injury initiated by a CXCR4-preferring gp120 we cross-bred CCR5-deficient mice with HIV gp120tg animals of two founder lines (4,5,12). The resulting two new mouse lines were viable and fertile and were designated as 'CCR5KO x HIVgp120tg mice', 'Line 1' and 'Line 2', respectively. Both mouse lines generated the four genotypes of interest to our study (CCR5$^{-/-}$ gp120$^+$ or 'CCR5KO x gp120'; CCR5$^{+/+}$ gp120$^+$ or 'gp120'; CCR5$^{+/+}$ gp120$^-$ or 'WT' and CCR5$^{-/-}$ gp120$^-$ or 'CCR5KO') at expected Mendelian ratios. At six months of age we harvested brain tissue and assessed injury of the CNS due to expression of gp120 in the presence and absence of CCR5. We immunolabeled neuronal dendrites for the marker microtubule-associated protein (MAP) 2 and presynaptic terminals for synaptophysin (Syp) in sagittal brain sections (Fig. 1*A*). Analysis using deconvolution microscopy in frontal cortex (layer 3) and hippocampus (molecular layer) showed that in both line 1 and 2, gp120 mice displayed a significant reduction in the percentage of neuropil positive for MAP-2 or Syp in comparison to all of the other three genotypes (Fig. 1*B, C*). The gp120 mice of line 2 showed significantly more loss of MAP-2$^+$ neuropil ($P < 0.01$) and a trend to less Syp ($P < 0.066$) in the cortex than their line 1 counterparts. Most notably for both lines, in the absence of CCR5 viral gp120 no longer caused a loss of neuronal dendrites and presynaptic terminals.

CCR5KO prevents microglial activation but not astrocytosis in HIV gp120tg brain

We next labeled sections for astrocytic GFAP or the microglial marker 'ionized calcium binding adaptor molecule 1' (Iba1) and used quantitative immunofluorescence microscopy

for analysis. Increased GFAP immunoreactivity indicating astrocytosis occurred in brains of gp120tg animals of both lines regardless of CCR5-deficiency, although in hippocampus of CCR5KO x gp120 mice of line 2, the increase of GFAP fluorescence did not reach significance (Fig. 1*D*). Of note, all animals of line 2 expressing gp120 showed significantly less astrocytosis in the cortex than their line 1 counterparts, independently of the CCR5 genotype ($P < 0.01$).

Counts of Iba1$^+$ cells indicated that gp120 mice displayed significantly more microglial cells than the three other genotypes, although there was a much smaller, yet significant increase of microglia in the hippocampus of CCR5KO x gp120 mice from line 1 (Fig. 1*E*). Also, CCR5KO x gp120 mice of line 2 displayed significantly lower numbers of Iba1$^+$ microglia than their WT controls. However, microglial cell numbers in lines 1 and 2 were not significantly different. Altogether, we concluded that in our mouse model CCR5 is required for HIVgp120 to cause microglial activation and neuronal damage but not to produce astrocytosis.

CCR5KO rescues spatial learning and memory in HIV gp120tg mice

Since gp120 mice of line 2 displayed the most pronounced loss of MAP-2$^+$ neuropil and synaptophysin in the cortex, we next subjected mice of this line to behavioral testing. The optomotor test of vision showed that all mice had intact vision and the light/dark transfer test found no differences between the genotypes. In the locomotor activity test, we detected a moderately significant effect of genotype on ambulation but not center activity or rearing behavior. Fisher's PLSD post hoc test revealed significantly lower levels of ambulation in CCR5KO, CCR5KO x gp120 and in gp120 mice relative to WT (Fig. 2*A*). Thus the loss of CCR5 (and to a lesser extent gp120 expression) was associated with decreased ambulatory but not center or rearing activity. Also, there was no evidence of either amelioration or exacerbation of the effect on ambulatory activity in the CCR5KO x gp120 mice.

The Barnes maze test revealed significant differences between gp120 mice and the other genotypes in three of four measures. Latencies to escape did drop across the blocks of three trials in all genotypes (Fig. 2*B*). The numbers of incorrect choices (errors) indicated a significant difference between WT and gp120 mice, with the latter making more errors in the final training trials (Fig. 2*C*). In the probe test following training, the WT, CCR5KO and CCR5KO x gp120 groups all spent significantly more time in the target quadrant of the maze relative to the average of time spent in the incorrect quadrants (Fig. 2*D*). Only gp120 mice failed to show this significant difference, suggesting that they lacked in the use of spatial cues to locate the escape chamber. Chi Square tests comparing each group to the WT group indicated that only the gp120 mice used significantly less spatial strategy on the final day of acquisition compared to WT control mice (Fig. 2*E*).

None of the behavioral tests showed any sex-dependent differences. Taken together, these data suggested that gp120 mice have impaired spatial learning and memory which is restored by genetic ablation of CCR5.

HIVgp120 affects gene expression in brains of CCR5WT and CCR5KO mice

In order to further characterize the neuroprotective effect of CCR5 ablation in the presence of HIVgp120, we next performed a microarray-based genome-wide gene expression analysis. We collected brain tissue and prepared whole brain RNA of all four genotypes at 1.5, 3, 6, 12, and 20 (line 1) or 16 months of age (line 2) in order to identify genes for which differential regulation may be affected by an interaction of HIVgp120 expression and age. GeneSpring GX12 expression analysis software was employed to carry out two-way ANOVAs looking at the variation in CNS gene expression as a function of mouse age and HIVgp120 genotype separately in CCR5WT and CCR5KO backgrounds and for lines 1 and 2 (Fig. 3*A*). Next we compared genes differentially expressed in association with the gp120[+] genotype or an interaction of age and gp120[+] genotype between the two mouse lines separately for the respective CCR5WT and CCR5KO (Fig. 3*B*). This approach indicated that the gp120[+] genotype of lines 1 and 2 shared 1195 differentially expressed genes in the presence of CCR5 and 1766 genes in the absence of the HIV co-receptor. A subsequent comparison of the two lists of shared genes identified a *core common set of genes* for mouse lines 1 and 2 comprising CCR5WT-specific, common (CCR5WT and KO) and CCR5KO-specific, differentially regulated genes that were represented by 734, 461 and 1305 gene probes, respectively (Supplemental Tables I*A*, *B* and II).

Shared differential gene expression in brains of HIVgp120tg mice and human HIV patients

Compared to the CCR5WT-specific and CCR5KO-specific, gp120 associated differentially expressed gene sets, the most pronounced differential regulation was observed in the CCR5WT/KO-common gene set, which also comprised the most up-regulated genes in the gp120-expressing brains of lines 1 and 2. HIVgp120^{+} brains of CCR5WT and KO and of both mouse lines displayed among the 10 most up-regulated genes C3, C4B/SLP, CXCL10, GFAP, GPNMB, LCN2 and LGALS3 at most time points (Supplemental Table II). Since five of these genes were recently reported to be differentially regulated in the brains of patients with HIV encephalitis (HIVE) and neurocognitive impairment (NCI) (31), we further investigated in how far the results from our microarray study recapitulated findings in human HIV patients. Differentially regulated human gene probes were matched with corresponding mouse probes and compared with the mouse brain arrays using GeneSpring GX12. Significant overlap was detected for differentially regulated genes in all three tested CNS regions of HIVE patients with NCI and the brains of CCR5WT and CCR5KO HIVgp120tg mice (Table II; for gene lists see Supplemental Table III).

HIVgp120 expression distinctly affects canonical pathways in the presence and absence of CCR5

In order to assess biological pathways associated with gp120-induced CNS injury and affected by CCR5 deficiency, we used IPA software to analyze how the differential gene expression patterns affected canonical signaling pathways. The three sets of differentially expressed genes all affected components of different canonical pathways (Table III and Fig. 4). Of note, the five highest scoring canonical pathways each for CCR5WT-specific and CCR5WT/KO common gene sets all belonged in the categories of immune system and inflammation (Fig. 4*A*–*J*). Notably, two of the five canonical pathways affected by

differential gene expression specific to CCR5WT explicitly implicated macrophages in gp120-associated neuronal injury and behavioral impairment (Fig. 4*A* and *E*). One pathway was specifically CCR5 signaling in macrophages. In contrast, CCR5KO-specific regulated pathways mapped to the nervous system, namely the γ-amino butyric acid (GABA) neurotransmission system and Huntington's Disease (HD, Fig. 4*K* and *N*), to basic physiological mechanisms (Fig. 4*M* and *O*) and one inflammation-related pathway (Fig. 4*L*).

CCR5WT-specific and CCR5WT/KO common gene sets showed primarily up-regulation of canonical pathway components for immunity and inflammation. In contrast, pathway components specifically affected by CCR5KO were more often down-regulated suggesting that activation of those pathways in association with gp120 expression may be ameliorated in the absence of the chemokine receptor.

Effect of CCR5KO on HIVgp120 expression

In order to explore possible explanations for the protective effect of CCR5-deficiency against gp120 neurotoxicity, we next investigated if CCR5-deficiency affected RNA expression of viral gp120. Quantitative reverse transcription polymerase chain reaction (qRT-PCR) revealed that expression of gp120 changed in an age-dependent fashion in both mouse lines, but with slightly different kinetics. The difference in gp120 RNA expression between line 1 and 2 (Fig. 5) may explain why line 2 animals showed a significant more pronounced loss of MAP-2 positive neuronal dendrites in cerebral cortex.

In contrast, qRT-PCR revealed age-dependent significant increases of CCR5 RNA expression in association with gp120 expression in both mouse lines (Fig. 6*A*, Supplemental Fig. 1*A*). Considering that the CCR5KO completely abrogated neuronal injury and behavioral impairment in our model, an increase of the chemokine receptor's expression presumably promoted the occurrence of neuropathology.

Effect of CCR5KO on other relevant host factors

Next we tested whether expression of the second HIV co-receptor, CXCR4, was affected by gp120 and CCR5-deficiency as suggested by the microarray (Supplemental Table I*A*). QRT-PCR showed that CXCR4 RNA was up-regulated in gp120tg brains of mouse lines 1 and 2, and CCR5-deficiency ameliorated that effect (Fig. 6*B*, Supplemental Fig. 1*B*).

CXCL12 is the natural ligand of CXCR4 and therefore could potentially compete with viral gp120 for the interaction with its receptor (1,8). QRT-PCR indicated minor age-dependent changes in CXCL12 RNA and no effect of CCR5-deficiency (Fig. 6*C*, Supplemental Fig. 1*C*).

QRT-PCR also revealed patterns of age-dependent and gp120-associated increases for RNA of CCL5, CCL2, CXCL10, C4b, LCN2 and less pronounced for CCL3 and CCL4 (Fig. 6*D–J*, Supplemental Fig. 1*D–J*). The absence of CCR5 showed effects only in some age groups. The increase of RNA expression in association with transgenic gp120 was higher in Line 2 compared to Line 1 for six of the 10 tested genes: CCR5, CCL2, CCL3 and CCL4 (in CCR5KO x gp120), CXCL10 and C4b. The changes in RNA were similar in both mouse lines for four genes: CXCR4, CXCL12/SDF-1, CCL5 and CCL4 (in CCR5WT). Only for

two genes, CCL4 (in CCR5WT) and LCN2, were increases in mRNA higher in Line 1 than Line 2. However, overall, the patterns of differential RNA expression were similar for the 10 genes in mouse lines 1 and 2.

LCN2, one of the most up-regulated proteins in gp120tg brains, and CCR5 have both been reported to affect the activation of macrophages and microglia. LCN2 was found to promote pro-inflammatory activation as well as apoptosis in microglia (22,23). CCR5-deficient macrophages reportedly displayed upon stimulation impaired cytokine production compared to their WT counterparts (4). Markers of microglia and macrophage activation can readily be detected in mRNA preparations from whole brain (23,34,35). In order to further explore the activation status of microglia in gp120tg brains, we analyzed the expression of genes that characterize classically activated macrophages (M1) and their alternatively activated counterparts (M2) (23,34,36,37). QRT-PCR showed an age-dependent increase of the M1 markers CD68 and TNFα that was more pronounced in gp120tg compared to control brains (Fig. 7*A, C*). CD68 was significantly higher in gp120tg samples than controls at 12 months, whereas the same pattern occurred with TNFα in the 1.5 months group. However, CCR5-deficiency made a significant difference for TNFα only between WT and the evenly higher expressing CCR5KO and CCR5KO x gp120 brains at 12 months of age. No significant changes were found in the expression of iNOS between the different genotypes or age groups (Fig. 7*B*).

In contrast, all three M2 markers showed gp120-associated alterations of expression in at least one age group (Fig. 7*D–F*). Arginase-1 (Arg-1) was significantly up-regulated in gp120tg brains compared to controls in both CCR5WT and KO backgrounds at 1.5 months (Fig. 7*D*). The same was true for CD163 at 6 months of age (Fig. 7*E*). MRC-1 expression was significantly increased in CCR5KO x gp120 compared to CCR5KO and WT brains at 1.5 and 6 months (Fig. 7*E*). In 6 months-old mice CCR5-deficiency made a difference in that expression of both CD163 and MRC-1 was increased in CCR5KO x gp120 compared to gp120 brains. Thus, despite a pronounced up-regulation of LCN2 in brains of gp120 and CCR5KO x gp120 mice, we found only in some age groups a slight increase of M1 markers CD68 and TNFα compared to controls. At the same time M2 markers were up-regulated in association gp120 expression, at least in 1.5 and 6 months old brains.

Increased expression of GFAP and LCN2 has been linked to astrocytosis (12,38–40). Our observations indicated that, in the presence of gp120, CCR5-deficiency protected neurons but left astrocytosis largely unchanged. In order to further explore the effect of CCR5KO on astrocytes, we analyzed in brain samples of Line 2 mice at 1.5, 6 and 12 months of age six additional astrocyte-specific factors that have been implicated in astrocytosis (40). GLAST and GLT1 are astrocytic glutamate transporters that play an important role in keeping the extracellular concentration of the major excitatory neurotransmitter at physiological, non-toxic levels (41). QRT-PCR indicated an overall age-dependent up-regulation of GLAST but not GLT1 in gp120tg brains in the presence and absence of CCR5. However, in 6 months-old animals expression of both transporters was significantly higher in CCR5KO x gp120 than gp120 mice (Fig. 8*A, B*). Ptx3 and TGM1 are in the brain specifically expressed in astrocytes (40). QRT-PCR showed an overall age-dependent up-regulation of both genes in gp120tg brains independent of the CCR5 genotype, although induction was up to about 50-

fold higher for TGM1 than Ptx3 (Fig. 8*C, D*). Astrocytes also produce soluble thrombospondins (Thbs) which support synaptogenesis (42). QRT-PCR revealed for Thbs1 an age-dependent increase within the gp120 mouse group, however the changes were overall not significant compared to WT mice. However, Thbs1 was significantly up-regulated at 1.5 month in CCR5KO x gp120 compared to the other three genotypes (Fig. 8*E*). In contrast, Thbs2 was significantly up-regulated in association with gp120 in both CCR5WT and KOs in an age-dependent fashion (Fig. 8*F*). Thus, overall CCR5-deficiency appeared to have limited effects on the increased expression of genes associated with astrocytosis in gp120tg brains.

Analysis of protein concentrations using an ELISA confirmed microarray and qRT-PCR results suggesting that LCN2 was highly up-regulated in gp120tg brain independently of CCR5 genotype (Fig. 9*A*, Supplemental Fig. 1*K*). Deconvolution microscopy confirmed that LCN2 was located to astrocytes (Fig. 9*B*). In contrast to LCN2, CXCL12 protein concentrations assessed by ELISA in extracts from brain tissues of 3, 6 and 12 months old mice differed from the mRNA expression pattern by showing significant reductions in association with gp120 expression in both mouse lines although at different ages (Fig. 9*C*, Supplemental Fig. 1*L*). CCR5-deficiency did not *per se* affect CXCL12 protein concentration but prevented a significant drop in HIVgp120tg brains except for the 12 months samples of line 2. ELISAs also confirmed significantly elevated protein levels for both CCL5 and -2 associated with gp120 expression (Fig. 9*D, E*). CCL5 protein was significantly more elevated in both mouse lines in the absence of CCR5, whereas the same effect occurred for CCL2 only in line 2.

LCN2 has been reported to stimulate an M1 polarization of microglia (23) and our qRT-PCR had detected increased mRNA for TNFα in gp120tg brains (Fig. 7). Therefore, we stained brain sections of all four genotypes of 6 months old Line 2 mice with a combination of antibodies against the microglial marker Iba1 and TNFα. In analogy to the quantitative fluorescence-based analysis of cell markers described above, Iba1 was used to generate masks defining microglial cell bodies in cerebral cortex and hippocampus and the fluorescence intensity for TNFα in microglial cells was estimated (Fig. 9*F* and *G*). Microglia in gp120tg brains showed a significantly higher fluorescence signal for TNFα in the presence and absence of CCR5 compared to WT controls. This observation was in line with an increased expression of a macrophage M1 marker in the presence of gp120 and LCN2, and indicated that microglial TNFα expression can occur in the absence of neuronal injury.

Altogether, the results indicated that the viral envelope protein gp120 can trigger components of an anti-viral innate immune response and astrocytosis independently of CCR5 genotype and neuronal injury.

CCR5KO abrogates accumulation of residential microglia in HIVgp120tg brain

Although immunofluorescence staining with Iba1 only indicated an increased number of microglia in gp120tg brain in the presence of CCR5, the strongly elevated CCL2 protein concentrations raised the question if any recruitment of peripheral mononuclear cells occurred. Therefore, we prepared live cell suspensions from whole brains of mice of all

genotypes from line 2 and analyzed cell surface expression of CD45 and CD11b by flow cytometry. Cells isolated from spleen served as controls (Fig. 9*H*). In brain CD11b$^+$CD45^{low} cells represent resident microglia/macrophages whereas CD11b$^+$CD45^{high} cells indicate recently infiltrated peripheral monocytes/macrophages (43). Quantification of CD11b$^+$CD45^{low} CNS cells indicated again that CCR5-deficiency was associated with a significant reduction of resident microglia/macrophages in gp120tg brain (Fig. 9*H*, upper panel, and *I*). The numbers of CD11b$^+$CD45^{high} cells in brain were comparably low with (in percent ± s.e.m.) 0.39 ± 0.28 (WT), 0.26 ± 0.11 (gp120), 0.49 ± 0.42 (CCR5KO) and 0.12 ± 0.04 (CCR5KO x gp120) and no significant differences between the genotypes. In contrast, CD11b$^+$CD45^{high} cells were readily detected in splenocyte populations (Fig. 9*H*, lower panel). Thus, increased levels of CCL2 and CCL5 were not associated with infiltration of peripheral CD11b$^+$CD45^{high} cells into the CNS while CCR5-deficiency appeared to restrict the number of CD11b$^+$CD45^{low} cells in gp120tg brains.

Interruption of CCR5 signaling and LCN2 cooperate to diminish microglial cell numbers and to protect neurons upon exposure to CXCR4-using HIVgp120

LCN2 has been reported to induce astrocytosis (39), pro-inflammatory activation as well as apoptosis in microglia (22,23) and to exert itself neurotoxicity (44). However, CCR5KO x gp120 mice express increased levels of LCN2 without showing neuronal injury suggesting that CCR5KO might also curb toxicity of LCN2. Therefore, we next assessed a potential functional link between LCN2 and CCR5 in the presence of a CXCR4-using viral gp120. We exposed cerebrocortical cell cultures derived from embryos of line 2 WT mice to gp120 of the CXCR4-utilizing HIV-1$_{IIIB}$ in the presence and absence of recombinant murine LCN2 or the CCR5 inhibitor Maraviroc (MVC), or combinations thereof, using published effective concentrations (14,33,44,45). Subsequent analysis of microglial and neuronal cell numbers by fluorescence microscopy showed that LCN2 and MVC in combination led to a significant increase of microglia. However, in the presence of the CXCR4-using gp120, LCN2 and MVC caused a significant reduction of microglial cells (Fig. 7*B*, *D*). The latter condition recapitulated the scenario in CCR5KO x gp120 mice. Moreover, gp120 and to a lesser extent LCN2 caused each a significant loss of neurons, although the combination did not significantly increase the toxicity of gp120. MVC alone abrogated the toxic effect of LCN2 but not of the CXCR4-using gp120. However, the combination of LCN2 and MVC completely prevented the loss of neurons in the presence of gp120, again recapitulating the observations in CCR5KO x gp120 mice, (Fig. 7*C, E*).

In analogy to the quantitative fluorescence-based analysis of TNFα in microglia in brain sections described above, Tomato lectin was used in separate experiments to define microglial cell bodies in cerebrocortical cell cultures. Afterwards, the fluorescence intensities for TNFα and ARG1 were estimated in microglia (Fig. 10*E*). Microglia in cerebrocortical cells exposed to LCN2 + MVC, with and without gp120, contained significantly more TNFα compared to vehicle controls. However, microglia in cerebrocortical cultures exposed to gp120 alone or the combination of MVC + LCN2 + gp120 showed significantly increased ARG1. Therefore, microglia simultaneously exposed to MVC + LCN2 + gp120 were reduced in numbers but expressed in comparison to vehicle controls increased levels of both TNFα and ARG1.

Discussion

Beyond its function as viral co-receptor, little is known about how CCR5 influences HIV-associated neurocognitive disorders. Here we show with histological analysis and behavioral testing that genetic ablation of CCR5 prevents neuronal injury, microglial activation, and impairment of spatial learning and memory in a transgenic mouse model expressing a CXCR4-utilizing HIVgp120 in the brain. These findings implied a crucial indirect role for the β-chemokine receptor in the *in vivo* brain damage mediated by the second viral co-receptor CXCR4.

Genetic CCR5-ablation also revealed that astrocytosis, another prominent pathological feature of AIDS brains (16,17,19), can occur independently from neuronal injury and behavioral impairment. Interestingly, gp120 mice of line 2 displayed significantly less MAP-2$^+$ neuropil and a trend to less Syp$^+$ presynaptic terminals in the cortex but also significantly less astrocytosis than their line 1 counterparts independently of the CCR5 genotype. Together with reports that in human HIV patients NCI can occur without HIVE, our findings raised the possibility that astrocytosis may reflect an insufficiently protective response of the CNS (31).

Genome-wide gene expression analysis of brains from all four genotypes of line 1 and 2 of CCR5KO x HIVgp120tg mice produced three major salient findings. First, a comparison of differentially regulated genes in brains of HIV patients with and without signs of HIVE and NCI (31) to those in gp120tg mouse brains revealed a significant overlap for both CCR5WT and KO. Thus, HIV gp120tg mice share not only significant neuropathological features but also a significant fraction of differentially expressed genes with brains of HIV and HIVE patients with NCI. Surprisingly, the human brain array did not report GFAP or LCN2 among the consistently up-regulated factors in HIVE patients although astrocytosis with increased GFAP immunoreactivity is one of the pathological hallmarks (16,17,19). A meta analysis of the human brain microarray data revealed that expression of GFAP and LCN2 was less consistent in human HIV/E brains than in the mouse model, but the expression of the two genes was highly correlated (Pearson r 0.6999; *P*-value < 0.0001). The potential contribution of the differentially regulated genes shared by HIV/E patients and HIVgp120tg mice to HIV neuropathogenesis will be the subject of further studies.

Second, the differential gene expression indicated that the viral envelope protein gp120 sufficed to trigger components of an innate immune response independently of the CCR5 genotype and neuronal injury. Some of the up-regulated factors had previously been implicated in HIV neuropathogenesis, such as CCL2, CCL5 and CXCL10 (46–52). However, in this study we investigated the potential role of LCN2, a 25 kDa soluble acute phase protein (39), which had not previously been implicated in HIV-associated brain injury. LCN2 was one of the most up-regulated immune factors in the brain of HIVgp120tg mice and will be discussed further below. The role of numerous other up- or down-regulated factors of the immune response in HIV neuropathogenesis remains to be elucidated.

Third, our microarray study allowed for identification of a *core common set of genes* for mouse lines 1 and 2 comprising genes that are differentially regulated in association with

viral gp120 expression in either a CCR5WT-specific, a common (CCR5WT and KO) or a CCR5KO-specific fashion. In HIVgp120tg mice the CCR5WT-specific genes were exclusively regulated in association with neuronal injury and behavioral disturbance. In contrast, CCR5WT/KO-common and CCR5KO-specific genes were differentially regulated independently of neuronal injury and compromised behavioral performance. Thus, differential expression of the CCR5WT/KO-common gene set may not suffice to mediate gp120-induced neuropathology and to compromise behavioral performance. Alternatively, the altered expression levels could reflect an attempt of the CNS to adapt to the presence of viral gp120 and protect against detrimental effects. The same might apply to the CCR5KO-specific pattern of differential gene expression. It remains to be elucidated for the CCR5WT-specific genes that were exclusively regulated in association with neuronal injury and behavioral disturbance, whether the differential regulation is a contributing cause or a consequence of HIVgp120-associated brain injury.

The CCR5WT/KO-common gene set contained GFAP and LCN2 among the most up-regulated genes in gp120tg brains and increased expression of both genes has been linked to astrocytosis (40). However, the gene expression pattern associated with astrocytosis can vary with the disease and the kind of brain injury. Different patterns have recently been described for example for middle cerebral artery occlusion (MCAO), mimicking a stroke, and intra-peritoneal injection of LPS, modeling a peripheral infection (40). LCN2 was the most up-regulated factor in both pathological models, and many of the same genes were significantly increased in MCAO, LPS exposure and in our model, although to different degrees. However, GFAP was relative to LCN2 far less increased after MCAO or LPS injection than in gp120tg mice, supporting the notion that different CNS diseases may evoke distinct astroglial responses. Besides GFAP and LCN2, we analyzed the expression of six additional astroglial genes by qRT-PCR, two astrocytic glutamate transporters, GLAST and GLT1 (41), two synaptogenesis promoting thrombospondins, Thbs1 and -2 (42), the acute phase protein Ptx3 (40) and the transglutaminase TGM1 (40). All these factors are of potential interest since HIV-1 and gp120-induced brain injury involve excitotoxicity mediated by glutamate receptors, oxidative stress, synaptic injury and inflammation (40). Five of the genes, GLAST, Ptx3, TGM1, Thbs1 and -2 showed significant differential regulation in association with gp120 expression at least in one age group, but CCR5-deficiency had a comparably small effect. GLT1 was reported to be unchanged in astrocytosis following MCAO or peripheral LPS injection (40), but our results suggested that it can change with astrogliosis in gp120tg brain in an age-dependent fashion. Also, GLAST was increased at 6 months in CCR5KO x gp120 compared to gp120 brains whereas CCR5-deficiency seemed to prevent a drop in GLT1 expression in gp120tg brain at the same age. Thus CCR5-deficiency might in an age-dependent manner favor an expression pattern of GLAST and GLT1 that prevents excitotoxic glutamate concentrations.

Altogether, our observations supported the notion that the overall neuroprotective deficiency of the chemokine receptor had limited effects on astrocytosis and only transiently affected glutamate transporters that are important to maintain non-toxic extracellular levels of the excitatory neurotransmitter.

Our recent *in vitro* studies showed that CCR5-deficient neurons are not *per se* protected against HIVgp120-induced toxicity of microglia and macrophages (14). In this study, CCR5-deficiency was not associated with a reduction of gp120 expression which could therefore not account for neuroprotection. However, since the transgenic mice express a CXCR4-using gp120 a reduced expression of CXCR4 could potentially contribute to the absence of neuronal damage in CCR5KO x gp120 mice, at least in line 1. Furthermore, we could not exclude that a less diminished CXCL12 concentration contributed at certain times to the neuroprotective effect of CCR5-ablation by reducing the availability of free CXCR4 to viral gp120.

Since CCR5KO x gp120 brains lacked neuronal injury, we could not strictly discern whether limitation of microglial cell numbers prevented neuronal damage or whether the absence of injured neurons abrogated the accumulation of microglia. In any case, ample published evidence supports a crucial role for macrophages and microglia in HIV-1 and gp120-induced neurotoxicity (33,48,56–60). The implication of microglia in gp120-induced neuronal injury *in vivo* is also in line with our finding of increased numbers of this cell type in cerebral cortex and hippocampus of gp120 mice. The possibility that CCR5-deficiency modulates *in vivo* the function of macrophages and microglia resulting in amelioration of gp120 neurotoxicity fits reports that CCR5-deficient macrophages show upon stimulation a diminished cytokine response compared to their WT counterparts (4). Moreover, our observation that CCR5KO x gp120 mice had a significantly reduced number of microglia compared to their CCR5WT gp120[+] counterparts despite the high expression of CCL2 and CCL5 is in line with a recent report that the CCL5-CCR5 axis is essential for survival of macrophages during viral infections (61).

In addition, the pattern of gene regulation specific to gp120tg brains expressing CCR5 explicitly implicated macrophages in two and CCR5 in one of the top five canonical pathways. Hence, the canonical pathways clearly linked CCR5 and macrophages/microglia to neuronal injury and behavioral impairment. Moreover, the top canonical pathway affected by the CCR5WT/KO common gene set represented communication between innate and adaptive immune cells and the fifth comprised TREM1 signaling, both of which suggested again the involvement of microglia and macrophages. Also, both CCR5WT-specific and CCR5WT/KO common gene sets pointed to up-regulation of immune activation and inflammation, but lacked a clear indication of a polarized activation of microglia and macrophages along the M1 and M2 spectrum (36,62). However, the CCR5WT/KO common gene set included significantly elevated CD86 and CXCL10, two markers of M1 polarization (36,62). Our analysis of three additional markers each for M1 and M2 polarization in three age groups indicated that gp120tg brains provided an environment where markers of both M1 and M2 type activation were up-regulated. Interestingly, CCR5-deficiency did not change that situation. Thus, microglia and macrophages in gp120tg brains may present with an intermediate phenotype on the M1–M2 spectrum (36,62) or comprise a mixed population of M1 and M2 polarized cells. A recent review of pathological mechanisms in HIV-1 and SIV infections suggested that M1 activation of macrophages and microglia predominates early while M2 type activation may prevail later in HIV-1 infection of the CNS (63). Microscopy-based quantification of microglial TNFα in mouse brain

sections overall confirmed the expression pattern indicated by qRT-PCR, although not all microglial cells appeared to have detectable levels of the cytokine. Future experiments will aim at a more detailed characterization of the microglial activation pattern in gp120tg brains.

CCR5KO x gp120 mice lacked any sign of behavioral impairment and neuronal injury. Canonical pathways specifically affected in CCR5KO-deficient gp120tg brains showed down-regulation of many pathway components, except for mineralocorticoid biosynthesis. The combined down-regulation of components of GABAergic neurotransmission, of endocytosis, of LPS/IL-1 mediated inhibition of a nuclear receptor and of an HD-associated signaling pathway suggested that significant adaptation of the CNS may be required to achieve neuroprotection in the presence of gp120.

LCN2 reportedly promotes pro-inflammatory activation as well as apoptosis in microglia (22) and has been linked to astrocytosis (39) and neurotoxicity (44). Thus, elevated LCN2 levels could presumably contribute to neuronal injury in gp120tg mice. However, we found that CCR5-deficiency allowed *in vivo* for high expression of LCN2 without neuronal injury and that *in vitro* inhibition of CCR5 blocked LCN2 neurotoxicity. Both findings suggested that the chemokine receptor was crucial for LCN2's neurotoxic effect.

Our experiments in cerebrocortical cell cultures revealed that LCN2 and interruption of CCR5 signaling paradoxically cooperated in the presence of a CXCR4-using HIVgp120 to reduce microglial cells in number and to protect neurons. Given the critical role of macrophages and microglia in HIV neurotoxicity, this observation provided an explanation and mechanism for *in vivo* protection against CXCR4-mediated gp120 neurotoxicity by CCR5-deficiency in our mouse model.

Quantification of TNFα and ARG1 in cerebrocortical microglia *in vitro* was overall in line with the RNA expression pattern seen in 1.5 months old mice, although the increase of the M1 marker TNFα following exposure to a combination of LCN2 and gp120 did not reach significance. Similarly, the increase of ARG1 between exposure to MVC and the combination of MVC + LCN2 + gp120 was not significant. However, the *in vitro* experiments showed that in a mixed neuronal-glial cell population LCN2 alone failed to increase microglial TNFα, although the acute phase protein caused neurotoxicity. However, the combination of CCR5 inhibition with MVC in combination with LCN2 showed a trend to increase the cytokine in microglia ($P = 0.078$) while also preventing neuronal loss. Thus, neurons and astrocytes as well as CCR5 blockade appeared to modulate the effect of LCN2 on microglia. The characterization of the exact cellular and molecular mechanism of this regulation will be the subject of future studies. Interestingly, gp120 triggered an increase of the M2 marker ARG1 in microglia, an effect that was ameliorated in the presence of either LCN2 ($P = 0.10$) or MVC alone but not their combination. Moreover, increased microglial ARG1 was associated with neurotoxicity. In contrast, microglial cells that remained after exposure to the neuroprotective combination of MVC + LCN2 + gp120 showed simultaneously elevated levels of TNFα and ARG1 thus recapitulating the mRNA expression pattern observed in brains of CCR5KO x gp120 mice.

In summary, we found *in vivo* evidence for a pathological role of CCR5 that appears to be independent of its co-receptor function since the gp120 in the transgenic mouse model uses CXCR4 (13). We also observed that neurotoxicity of LCN2 is CCR5-dependent, and pharmacologically abrogating CCR5 signaling revealed a novel protective effect of LCN2 in HIV/gp120-associated brain injury and behavioral impairment. Considering that transgenic mice are a model with limitations and gp120 is only one of several HIV components that can cause neuronal injury, our findings nevertheless raise the possibility that inhibition of CCR5 might be beneficial against HIV-associated CNS injury even in the presence of a CXCR4-using virus.

Supplementary Material

Refer to Web version on PubMed Central for supplementary material.

Acknowledgments

Abbreviations used in this paper

ANI	HIV-1-associated asymptomatic neurocognitive impairment
HAND	HIV-1 associated neurocognitive disorders
HAD	HIV-associated dementia
HIVE	HIV encephalitis
MND	HIV-1-associated mild neurocognitive disorder
NCI	neurocognitive impairment

References

1. Michael NL, Moore JP. HIV-1 entry inhibitors: Evading the issue. Nat Med. 1999; 5:740–742. [PubMed: 10395316]

2. Dean M, Carrington M, Winkler C, Huttley GA, Smith MW, Allikmets R, Goedert JJ, Buchbinder SP, Vittinghoff E, Gomperts E, Donfield S, Vlahov D, Kaslow R, Saah A, Rinaldo C, Detels R, O'Brien SJ. Genetic restriction of HIV-1 infection and progression to AIDS by a deletion allele of the CKR5 structural gene. Hemophilia Growth and Development Study, Multicenter AIDS Cohort Study, Multicenter Hemophilia Cohort Study, San Francisco City Cohort, ALIVE Study. Science. 1996; 273:1856–1862. [PubMed: 8791590]

3. Cordelier P, Morse B, Strayer DS. Targeting CCR5 with siRNAs: using recombinant SV40-derived vectors to protect macrophages and microglia from R5-tropic HIV. Oligonucleotides. 2003; 13:281–294. [PubMed: 15000819]

4. Zhou Y, Kurihara T, Ryseck RP, Yang Y, Ryan C, Loy J, Warr G, Bravo R. Impaired macrophage function and enhanced T cell-dependent immune response in mice lacking CCR5 the mouse homologue of the major HIV-1 coreceptor. J Immunol. 1998; 160:4018–4025. [PubMed: 9558111]

5. Huffnagle GB, McNeil LK, McDonald RA, Murphy JW, Toews GB, Maeda N, Kuziel WA. Cutting edge: Role of C-C chemokine receptor 5 in organ-specific and innate immunity to Cryptococcus neoformans. J Immunol. 1999; 163:4642–4646. [PubMed: 10528159]

6. Cocchi F, Devico AL, Garzino-Demo A, Arya SK, Gallo RC, Lusso P. Identification of RANTES, MIP-1 alpha, and MIP-1 beta as the major HIV- suppressive factors produced by CD8+ T cells. Science. 1995; 270:1811–1815. [PubMed: 8525373]

7. Dolan MJ, Kulkarni H, Camargo JF, He W, Smith A, Anaya JM, Miura T, Hecht FM, Mamtani M, Pereyra F, Marconi V, Mangano A, Sen L, Bologna R, Clark RA, Anderson SA, Delmar J, O'connell RJ, Lloyd A, Martin J, Ahuja SS, Agan BK, Walker BD, Deeks SG, Ahuja SK. CCL3L1 and CCR5 influence cell-mediated immunity and affect HIV-AIDS pathogenesis via viral entry-independent mechanisms. Nat Immunol. 2007; 8:1324–1336. [PubMed: 17952079]

8. Kaul M, Garden GA, Lipton SA. Pathways to neuronal injury and apoptosis in HIV-associated dementia. Nature. 2001; 410:988–994. [PubMed: 11309629]

9. Gorry PR, Bristol G, Zack JA, Ritola K, Swanstrom R, Birch CJ, Bell JE, Bannert N, Crawford K, Wang H, Schols D, De Clercq E, Kunstman K, Wolinsky SM, Gabuzda D. Macrophage tropism of human immunodeficiency virus type 1 isolates from brain and lymphoid tissues predicts neurotropism independent of coreceptor specificity. J Virol. 2001; 75:10073–10089. [PubMed: 11581376]

10. Kramer-Hammerle S, Rothenaigner I, Wolff H, Bell JE, Brack-Werner R. Cells of the central nervous system as targets and reservoirs of the human immunodeficiency virus. Virus Res. 2005; 111:194–213. [PubMed: 15885841]

11. Lindl KA, Marks DR, Kolson DL, Jordan-Sciutto KL. HIV-associated neurocognitive disorder: pathogenesis and therapeutic opportunities. J Neuroimmune Pharmacol. 2010; 5:294–309. [PubMed: 20396973]

12. Toggas SM, Masliah E, Rockenstein EM, Rall GF, Abraham CR, Mucke L. Central nervous system damage produced by expression of the HIV-1 coat protein gp120 in transgenic mice. Nature. 1994; 367:188–193. [PubMed: 8114918]

13. Valentin A, Trivedi H, Lu W, Kostrikis LG, Pavlakis GN. CXCR4 mediates entry and productive infection of syncytia-inducing (X4) HIV-1 strains in primary macrophages. Virology. 2000; 269:294–304. [PubMed: 10753708]

14. Kaul M, Ma Q, Medders KE, Desai MK, Lipton SA. HIV-1 coreceptors CCR5 and CXCR4 both mediate neuronal cell death but CCR5 paradoxically can also contribute to protection. Cell Death Differ. 2007; 14:296–305. [PubMed: 16841089]

15. Lee MH, Wang T, Jang MH, Steiner J, Haughey N, Ming GL, Song H, Nath A, Venkatesan A. Rescue of adult hippocampal neurogenesis in a mouse model of HIV neurologic disease. Neurobiol Dis. 2011; 41:678–687. [PubMed: 21146610]

16. Budka H. Neuropathology of human immunodeficiency virus infection. Brain Pathol. 1991; 1:163–175. [PubMed: 1669705]

17. Brew BJ, Rosenblum M, Cronin K, Price RW. AIDS dementia complex and HIV-1 brain infection: clinical-virological correlations. Ann Neurol. 1995; 38:563–570. [PubMed: 7574452]

18. Bandaru VV, Patel N, Ewaleifoh O, Haughey NJ. A failure to normalize biochemical and metabolic insults during morphine withdrawal disrupts synaptic repair in mice transgenic for HIV-gp120. J Neuroimmune Pharmacol. 2011; 6:640–649. [PubMed: 21748284]

19. Kolson DL. Neuropathogenesis of central nervous system HIV-1 infection. Clin Lab Med. 2002; 22:703–717. [PubMed: 12244593]

20. Krucker T, Toggas SM, Mucke L, Siggins GR. Transgenic mice with cerebral expression of human immunodeficiency virus type-1 coat protein gp120 show divergent changes in short- and long-term potentiation in CA1 hippocampus. Neuroscience. 1998; 83:691–700. [PubMed: 9483553]

21. D'hooge R, Franck F, Mucke L, De Deyn PP. Age-related behavioural deficits in transgenic mice expressing the HIV-1 coat protein gp120. Eur J Neurosci. 1999; 11:4398–4402. [PubMed: 10594667]

22. Lee S, Lee J, Kim S, Park JY, Lee WH, Mori K, Kim SH, Kim IK, Suk K. A dual role of lipocalin 2 in the apoptosis and deramification of activated microglia. J Immunol. 2007; 179:3231–3241. [PubMed: 17709539]

23. Jang E, Lee S, Kim JH, Kim JH, Seo JW, Lee WH, Mori K, Nakao K, Suk K. Secreted protein lipocalin-2 promotes microglial M1 polarization. FASEB J. 2013; 27:1176–1190. [PubMed: 23207546]

24. Crawley JN. Behavioral phenotyping of transgenic and knockout mice: experimental design and evaluation of general health, sensory functions, motor abilities, and specific behavioral tests. Brain Res. 1999; 835:18–26. [PubMed: 10448192]

25. Wang J, Dunn AJ, Roberts AJ, Zhang H. Decreased immobility in swimming test by homologous interferon-alpha in mice accompanied with increased cerebral tryptophan level and serotonin turnover. Neurosci Lett. 2009; 452:96–100. [PubMed: 19383422]

26. Roberts AJ, Maung R, Sejbuk NE, Ake C, Kaul M. Alteration of Methamphetamine-induced stereotypic behaviour in transgenic mice expressing HIV-1 envelope protein gp120. J Neurosci Methods. 2009; 186:222–225.10.1016/j.jneumeth.2009.11.007 [PubMed: 19917310]

27. Barnes CA. Memory deficits associated with senescence: a neurophysiological and behavioral study in the rat. J Comp Physiol Psychol. 1979; 93:74–104. [PubMed: 221551]

28. Bach ME, Hawkins RD, Osman M, Kandel ER, Mayford M. Impairment of spatial but not contextual memory in CaMKII mutant mice with a selective loss of hippocampal LTP in the range of the theta frequency. Cell. 1995; 81:905–915. [PubMed: 7781067]

29. Kunz S, Rojek JM, Roberts AJ, McGavern DB, Oldstone MB, de la Torre JC. Altered central nervous system gene expression caused by congenitally acquired persistent infection with lymphocytic choriomeningitis virus. J Virol. 2006; 80:9082–9092. [PubMed: 16940520]

30. Garden GA, Budd SL, Tsai E, Hanson L, Kaul M, D'Emilia DM, Friedlander RM, Yuan J, Masliah E, Lipton SA. Caspase cascades in human immunodeficiency virus-associated neurodegeneration. J Neurosci. 2002; 22:4015–4024. [PubMed: 12019321]

31. Gelman BB, Chen T, Lisinicchia JG, Soukup VM, Carmical JR, Starkey JM, Masliah E, Commins DL, Brandt D, Grant I, Singer EJ, Levine AJ, Miller J, Winkler JM, Fox HS, Luxon BA, Morgello S. The National NeuroAIDS Tissue Consortium brain gene array: two types of HIV-associated neurocognitive impairment. PLoS ONE. 2012; 7:e46178. [PubMed: 23049970]

32. Nichols JR, Aldrich AL, Mariani MM, Vidlak D, Esen N, Kielian T. TLR2 deficiency leads to increased Th17 infiltrates in experimental brain abscesses. J Immunol. 2009; 182:7119–7130. [PubMed: 19454709]

33. Medders KE, Sejbuk NE, Maung R, Desai MK, Kaul M. Activation of p38 MAPK is required in monocytic and neuronal cells for HIV glycoprotein 120-induced neurotoxicity. J Immunol. 2010; 185:4883–4895. [PubMed: 20855878]

34. Kigerl KA, Gensel JC, Ankeny DP, Alexander JK, Donnelly DJ, Popovich PG. Identification of two distinct macrophage subsets with divergent effects causing either neurotoxicity or regeneration in the injured mouse spinal cord. J Neurosci. 2009; 29:13435–13444. [PubMed: 19864556]

35. Chiu IM, Morimoto ET, Goodarzi H, Liao JT, O'Keeffe S, Phatnani HP, Muratet M, Carroll MC, Levy S, Tavazoie S, Myers RM, Maniatis T. A neurodegeneration-specific gene-expression signature of acutely isolated microglia from an amyotrophic lateral sclerosis mouse model. Cell Rep. 2013; 4:385–401. [PubMed: 23850290]

36. Gordon S, Taylor PR. Monocyte and macrophage heterogeneity. Nat Rev Immunol. 2005; 5:953–964. [PubMed: 16322748]

37. Kobayashi K, Imagama S, Ohgomori T, Hirano K, Uchimura K, Sakamoto K, Hirakawa A, Takeuchi H, Suzumura A, Ishiguro N, Kadomatsu K. Minocycline selectively inhibits M1 polarization of microglia. Cell Death Dis. 2013; 4:e525. [PubMed: 23470532]

38. Hatfield JS, Skoff RP. GFAP immunoreactivity reveals astrogliosis in females heterozygous for jimpy. Brain Res. 1982; 250:123–131. [PubMed: 6291720]

39. Lee S, Park JY, Lee WH, Kim H, Park HC, Mori K, Suk K. Lipocalin-2 is an autocrine mediator of reactive astrocytosis. J Neurosci. 2009; 29:234–249. [PubMed: 19129400]

40. Zamanian JL, Xu L, Foo LC, Nouri N, Zhou L, Giffard RG, Barres BA. Genomic analysis of reactive astrogliosis. J Neurosci. 2012; 32:6391–6410. [PubMed: 22553043]

41. Gegelashvili G, Danbolt NC, Schousboe A. Neuronal soluble factors differentially regulate the expression of the GLT1 and GLAST glutamate transporters in cultured astroglia. J Neurochem. 1997; 69:2612–2615. [PubMed: 9375696]

42. Christopherson KS, Ullian EM, Stokes CC, Mullowney CE, Hell JW, Agah A, Lawler J, Mosher DF, Bornstein P, Barres BA. Thrombospondins are astrocyte-secreted proteins that promote CNS synaptogenesis. Cell. 2005; 120:421–433. [PubMed: 15707899]

43. Sedgwick JD, Schwender S, Imrich H, Dorries R, Butcher GW, ter Meulen V. Isolation and direct characterization of resident microglial cells from the normal and inflamed central nervous system. Proc Natl Acad Sci U S A. 1991; 88:7438–7442. [PubMed: 1651506]

44. Bi F, Huang C, Tong J, Qiu G, Huang B, Wu Q, Li F, Xu Z, Bowser R, Xia XG, Zhou H. Reactive astrocytes secrete lcn2 to promote neuron death. Proc Natl Acad Sci U S A. 2013; 110:4069–4074. [PubMed: 23431168]

45. Dorr P, Westby M, Dobbs S, Griffin P, Irvine B, Macartney M, Mori J, Rickett G, Smith-Burchnell C, Napier C, Webster R, Armour D, Price D, Stammen B, Wood A, Perros M. Maraviroc (UK-427,857), a potent, orally bioavailable, and selective small-molecule inhibitor of chemokine receptor CCR5 with broad-spectrum anti-human immunodeficiency virus type 1 activity. Antimicrob Agents Chemother. 2005; 49:4721–4732. [PubMed: 16251317]

46. Dhillon NK, Williams R, Callen S, Zien C, Narayan O, Buch S. Roles of MCP-1 in development of HIV-dementia. Front Biosci. 2008; 13:3913–3918. [PubMed: 18508485]

47. Sanders VJ, Pittman CA, White MG, Wang G, Wiley CA, Achim CL. Chemokines and receptors in HIV encephalitis. AIDS. 1998; 12:1021–1026. [PubMed: 9662198]

48. Kaul M, Lipton SA. Chemokines and activated macrophages in HIV gp120-induced neuronal apoptosis. Proc Natl Acad Sci U S A. 1999; 96:8212–8216. [PubMed: 10393974]

49. Letendre SL, Lanier ER, McCutchan JA. Cerebrospinal fluid beta chemokine concentrations in neurocognitively impaired individuals infected with human immunodeficiency virus type 1. J Infect Dis. 1999; 180:310–319. [PubMed: 10395844]

50. Meucci O, Fatatis A, Simen AA, Bushell TJ, Gray PW, Miller RJ. Chemokines regulate hippocampal neuronal signaling and gp120 neurotoxicity. Proc Natl Acad Sci U S A. 1998; 95:14500–14505. [PubMed: 9826729]

51. Zink MC, Coleman GD, Mankowski JL, Adams RJ, Tarwater PM, Fox K, Clements JE. Increased macrophage chemoattractant protein-1 in cerebrospinal fluid precedes and predicts simian immunodeficiency virus encephalitis. J Infect Dis. 2001; 184:1015–1021. [PubMed: 11574916]

52. Sui Y, Stehno-Bittel L, Li S, Loganathan R, Dhillon NK, Pinson D, Nath A, Kolson D, Narayan O, Buch S. CXCL10-induced cell death in neurons: role of calcium dysregulation. Eur J Neurosci. 2006; 23:957–964. [PubMed: 16519660]

53. Flower DR, North AC, Attwood TK. Structure and sequence relationships in the lipocalins and related proteins. Protein Sci. 1993; 2:753–761. [PubMed: 7684291]

54. Rodriguez-Grande B, Swana M, Nguyen L, Englezou P, Maysami S, Allan SM, Rothwell NJ, Garlanda C, Denes A, Pinteaux E. The acute-phase protein PTX3 is an essential mediator of glial scar formation and resolution of brain edema after ischemic injury. J Cereb Blood Flow Metab. 2014; 34:480–488. [PubMed: 24346689]

55. Kraft-Terry SD, Buch SJ, Fox HS, Gendelman HE. A coat of many colors: neuroimmune crosstalk in human immunodeficiency virus infection. Neuron. 2009; 64:133–145. [PubMed: 19840555]

56. Koenig S, Gendelman HE, Orenstein JM, Dal Canto MC, Pezeshkpour GH, Yungbluth M, Janotta F, Aksamit A, Martin MA, Fauci AS. Detection of AIDS virus in macrophages in brain tissue from AIDS patients with encephalopathy. Science. 1986; 233:1089–1093. [PubMed: 3016903]

57. Giulian D, Vaca K, Noonan CA. Secretion of neurotoxins by mononuclear phagocytes infected with HIV-1. Science. 1990; 250:1593–1596. [PubMed: 2148832]

58. Meucci O, Miller RJ. Gp120-induced neurotoxicity in hippocampal pyramidal neuron cultures: protective action of TGF-beta1. J Neurosci. 1996; 16:4080–4088. [PubMed: 8753870]

59. O'Donnell LA, Agrawal A, Jordan-Sciutto KL, Dichter MA, Lynch DR, Kolson DL. Human immunodeficiency virus (HIV)-induced neurotoxicity: roles for the NMDA receptor subtypes. J Neurosci. 2006; 26:981–990. [PubMed: 16421318]

60. Choi WT, Kaul M, Kumar S, Wang J, Kumar IM, Dong CZ, An J, Lipton SA, Huang Z. Neuronal apoptotic signaling pathways probed and intervened by synthetically and modularly modified (SMM) chemokines. J Biol Chem. 2007; 282:7154–7163. [PubMed: 17218311]

61. Tyner JW, Uchida O, Kajiwara N, Kim EY, Patel AC, O'sullivan MP, Walter MJ, Schwendener RA, Cook DN, Danoff TM, Holtzman MJ. CCL5-CCR5 interaction provides antiapoptotic signals for macrophage survival during viral infection. Nat Med. 2005; 11:1180–1187. [PubMed: 16208318]

62. Mosser DM, Edwards JP. Exploring the full spectrum of macrophage activation. Nat Rev Immunol. 2008; 8:958–969. [PubMed: 19029990]

63. Burdo TH, Lackner A, Williams KC. Monocyte/macrophages and their role in HIV neuropathogenesis. Immunol Rev. 2013; 254:102–113. [PubMed: 23772617]
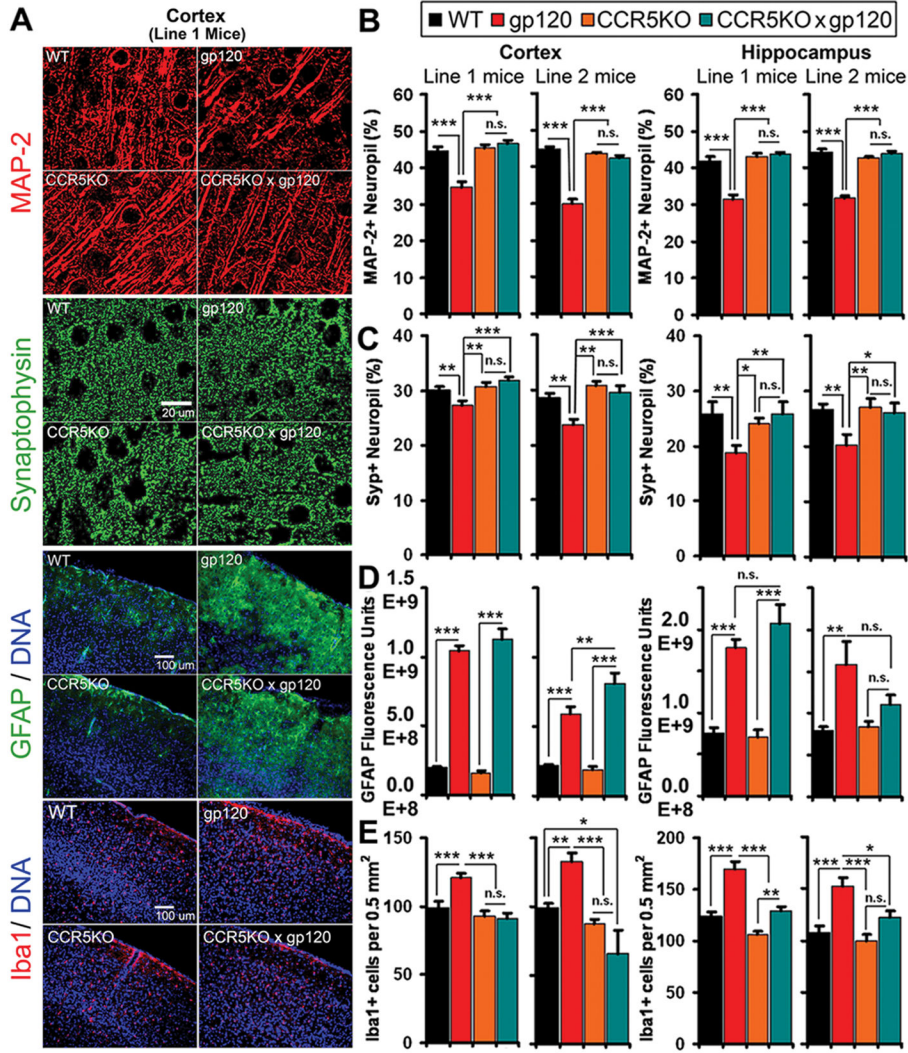
FIGURE 1.
CCR5-deficiency prevents neuronal damage and limits microglial activation but does not abrogate astrocytosis in HIV gp120tg mice. *A,* Representative images of frontal cerebral cortex immunolabeled for neuronal MAP-2 and synaptophysin (Syp; layer III, deconvolution microscopy, upper two panels; scale bar, 20 μm) and astrocytic GFAP (in green, DNA in blue, fluorescence microscopy, second panel from bottom) and microglial Iba1 (red, DNA in blue, bottom panel). *B – E,* Quantification of microscopy data obtained in frontal cortex and hippocampus of sagittal brain sections of six months old HIVgp120tg mice and controls expressing or lacking CCR5: *B,* Neuropil positive for neuronal MAP-2 and, *C,* Syp in percent positive neuropil; *D,* Fluorescence signal for astrocytic GFAP (arbitrary units); *E,* Quantification of Iba1^{+} microglia. Counts of Iba1^{+} microglia were obtained on three sagittal sections per animal and the three sections represented brain areas spaced 300 μm apart medial to lateral. Values are mean ± s.e.m. (*** $P < 0.001$, ** $P < 0.01$, * $P < 0.05$; ANOVA and Fisher's PLSD post hoc test; n = 3 – 4 animals per group/genotype; n.s., not significant).
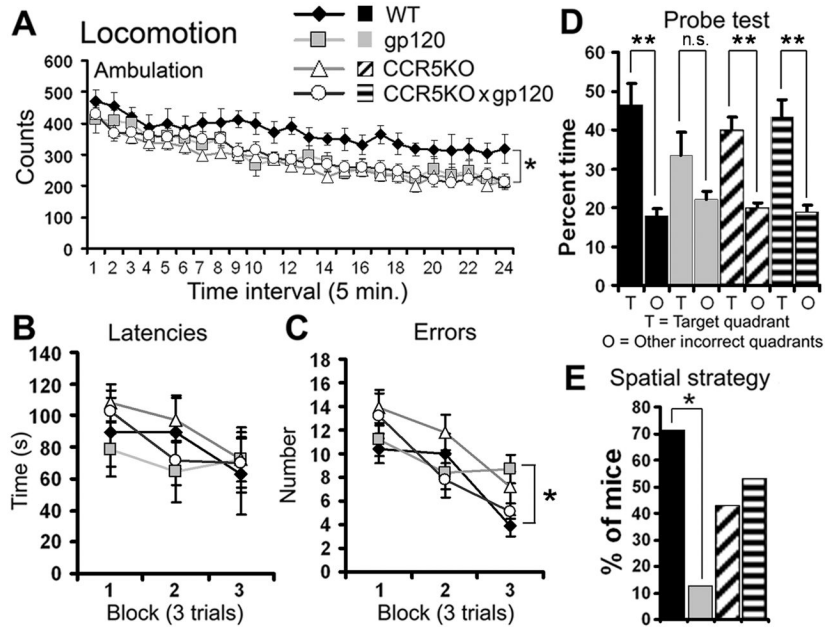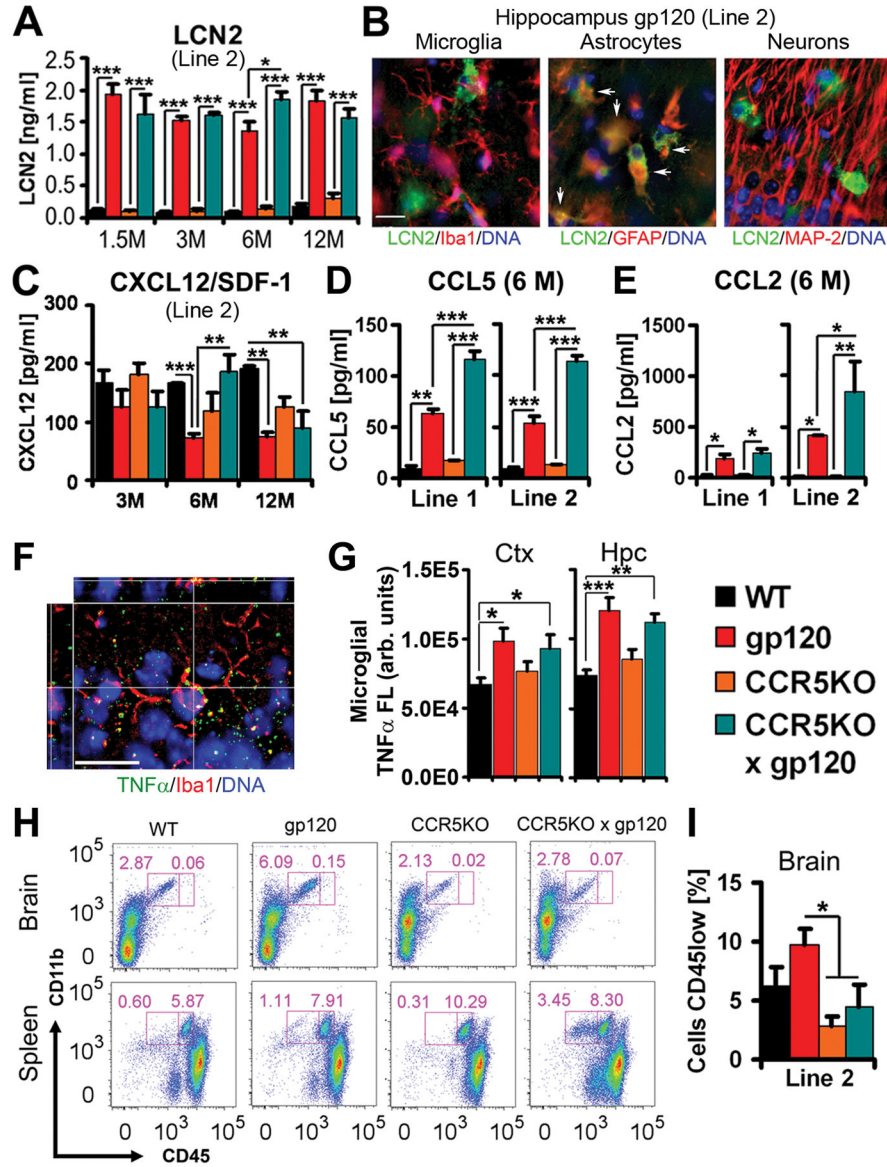
FIGURE 2.
CCR5-deficiency protects spatial learning and memory performance in HIVgp120tg mice. *A*, Locomotion (Ambulation), ANOVA and Fisher's PLSD post hoc test; * $P < 0.007$ (CCR5KO), $P < 0.03$ (CCR5KO x gp120), $P < 0.05$ (gp120) compared to WT. *B –E*, Barnes Maze test for spatial learning and memory; *B*, Latencies, *C*, Errors, *D*, Probe test, *E*, Spatial strategy; ANOVA and Fisher's PLSD post hoc test, Latencies, $P < 0.26$; Errors, * $P < 0.03$ for gp120 compared to WT; Probe test, ** P 0.003 (WT), $P < 0.0002$ (CCR5KO), $P < 0.0012$ (CCR5 KO x gp120); Spatial strategy, $\chi^2 = 5.4$, * $P < 0.02$ for gp120 compared to WT. Eight to nine months old gp120 (n = 9), CCR5KO x gp120tg mice (n = 17) and WT (n = 8) and CCR5KO control (n = 21) animals of line 2 were studied using the indicated behavioral tests. Values are mean ± s.e.m. (*A–D*) or mean (*E*); n.s., not significant.
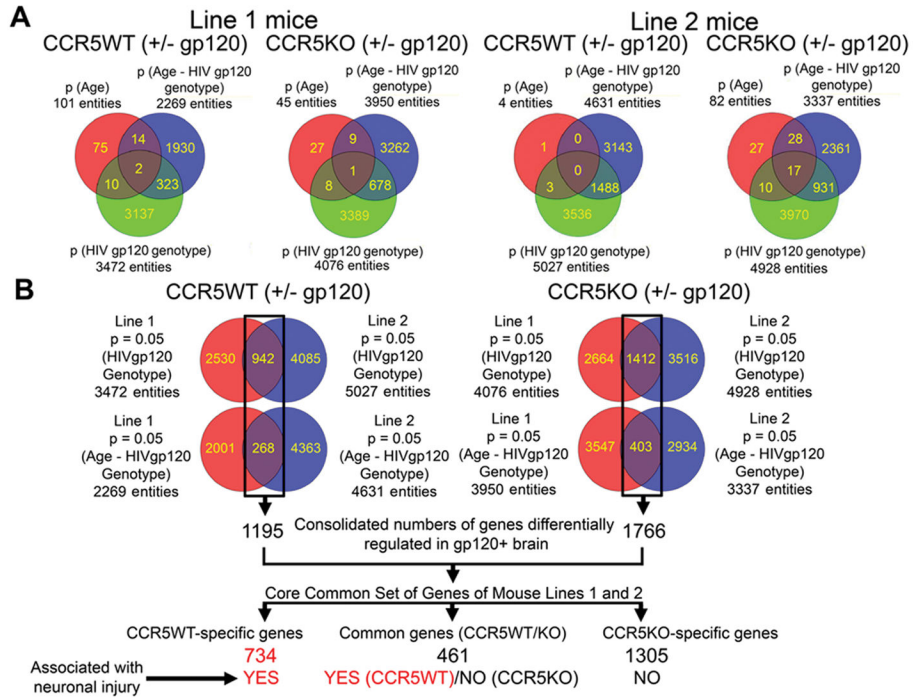
FIGURE 3.

Genome-wide gene expression analysis for brain identifies a core common set of genes for mouse lines 1 and 2. *A*, Two-way ANOVA of gene expression data obtained by microarray with whole brain RNA of gp120, CCR5KO x gp120 mice and WT and CCR5KO control animals of lines 1 and 2, respectively, at five different time points (1.5, 3, 6, 12, and 20 (line 1) or 16 (line 2) of age; n = 3 – 8 per genotype and age group); *B*, Identification of a *core common set of genes* for mouse lines 1 and 2 from overlap in differentially expressed genes due to HIVgp120tg genotype or an interaction of age and gp120^{+} genotype in the presence (left panel) and absence of CCR5 (right panel). The resulting lists of CCR5WT-specific, Common and CCR5KO-specific genes are represented by 734, 461 and 1305 probes, respectively.
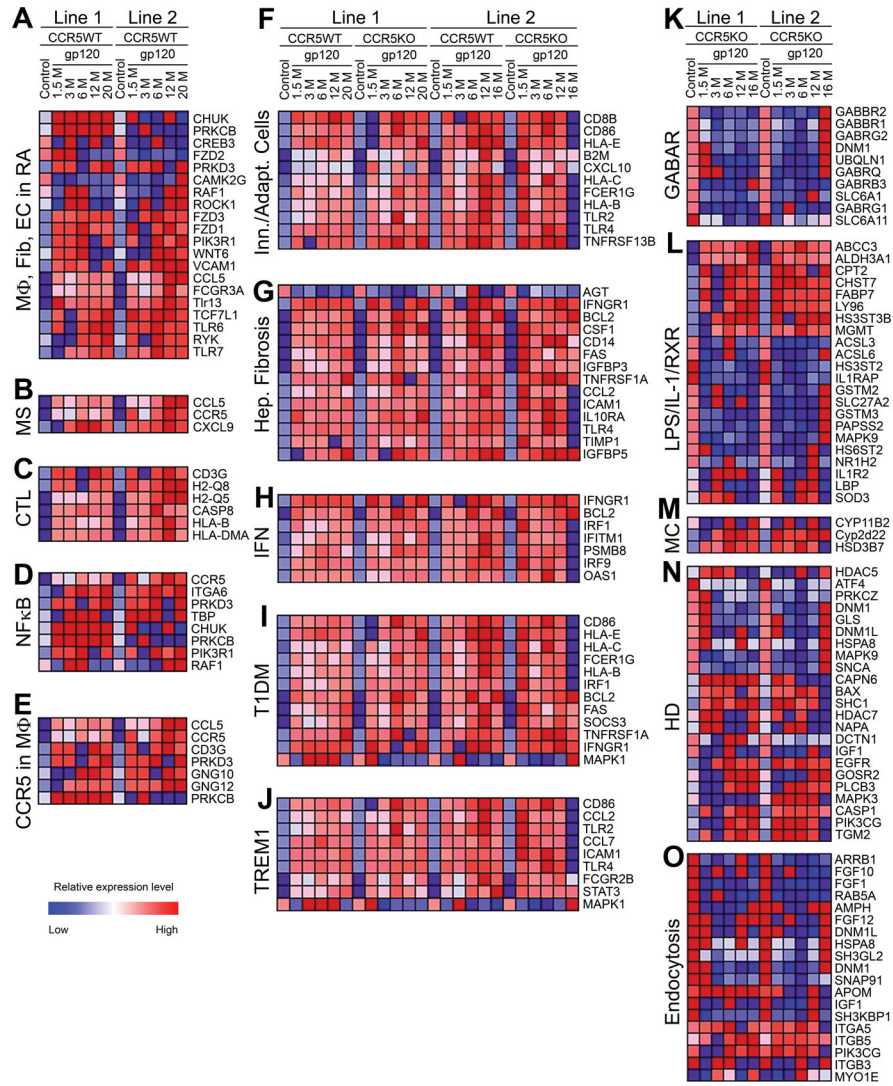
FIGURE 4.
Canonical pathways affected by differential expression of the core of common set of genes. CCR5WT HIVgp120tg mice of lines 1 and 2: **A,** Role of Macrophages, Fibroblasts and Endothelial Cells in Rheumatoid Arthritis (MΦ, Fib, EC in RA); **B,** Pathogenesis of Multiple Sclerosis (MS); **C,** Cytotoxic T Lymphocyte-mediated Apoptosis of Target Cells (CTL); **D,** NFkB Activation by Viruses (NFkB); **E,** CCR5 Signaling in Macrophages (CCR5 in MΦ). CCR5WT & KO HIVgp120tg mice of lines 1 and 2: **F,** Communication between Innate and Adaptive Immune Cells (Inn./Adapt. Cells); **G,** Hepatic Fibrosis / Hepatic Stellate Cell Activation (Hep. Fibrosis); **H,** Interferon Signaling (IFN); **I,** Type I Diabetes Mellitus Signaling (T1DM); **J,** Triggering Receptor Expressed on Monocytes/Myeloid cells 1 (TREM1) Signaling. CCR5KO HIVgp120tg mice of lines 1 and 2: **K,** GABA Receptor Signaling (GABAR); **L,** LPS/IL-1 Mediated Inhibition of RXR Function (LPS/IL-1/RXR); **M,** Mineralocorticoid Biosynthesis (MC); **N,** Huntington's Disease Signaling (HD); **O,** Clathrin-mediated Endocytosis Signaling (Endocytosis). See Table III for *P*-values, number of molecules affected, molecules in pathway and ratio. The data were filtered on fold-change

across the time course by using the online tool and database of IPA for canonical pathways. Based on the filter results, gene lists were generated for mouse lines 1 and 2 and their expression patterns are shown as heatmaps, which were produced using the tool HierarchicalClusteringImage and the default color map of GenePattern 3.5.0 software (Broad Institute) with the data being hierarchically clustered by rows and row normalized. The 'control' columns represent the normalized expression levels for the genes in the respective WT/CCR5KO controls.
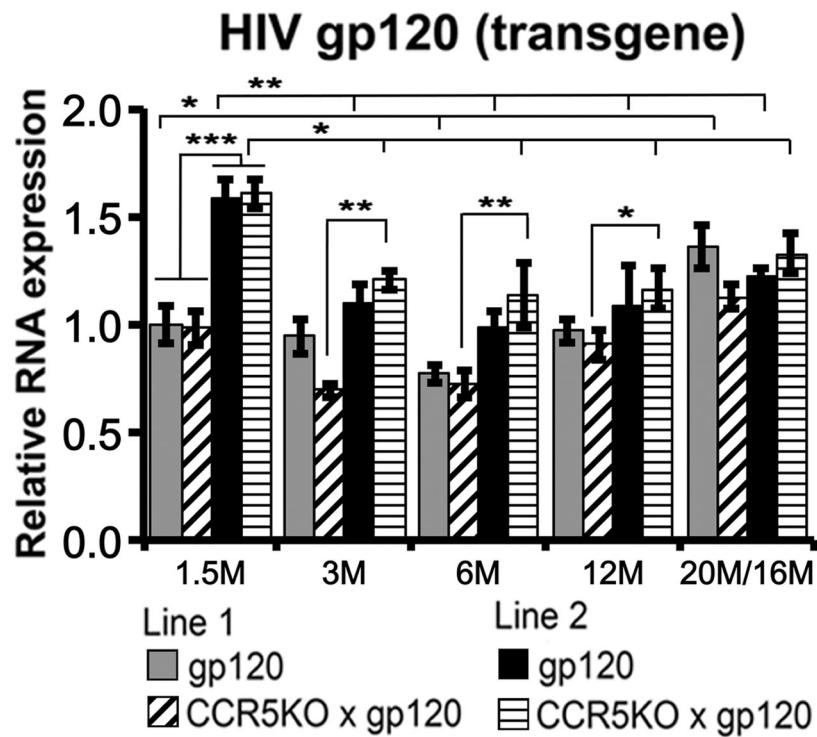
FIGURE 5.
RNA expression of HIVgp120 in the CNS in the presence and absence of CCR5. RNA preparation and qRT-PCR analysis was performed as described in Materials and Methods. Values are mean ± s.e.m. (*** $P < 0.001$, ** $P < 0.01$, * $P < 0.05$; ANOVA and Fisher's PLSD post hoc test; n = 3 – 6 animals per group/genotype).
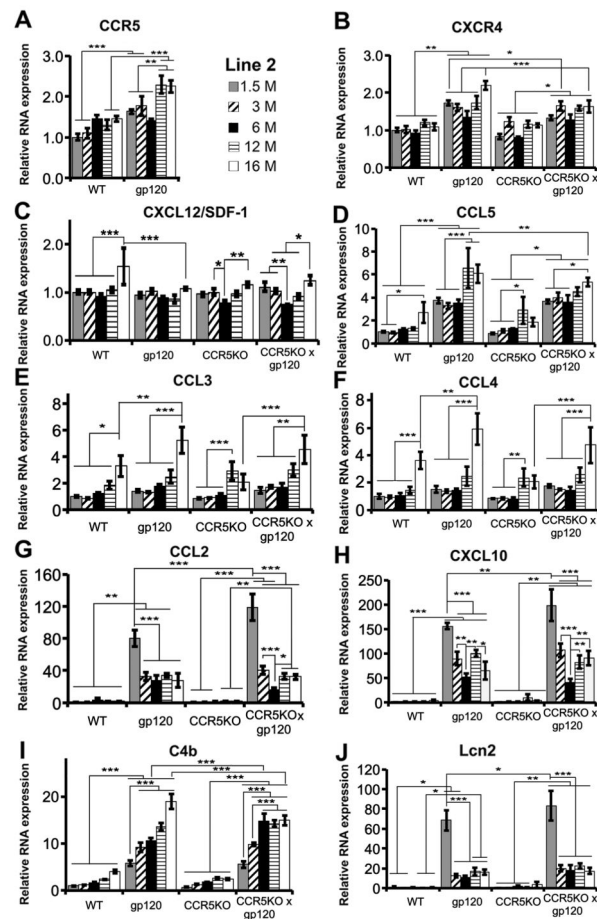
FIGURE 6.
Effect of CCR5-deficiency on RNA expression of host factors in the CNS. Analysis of mRNA expression in brain of Line 2 mice using quantitative RT-PCR: *A*, CCR5; *B*, CXCR4; *C*, CXCL12; *D*, CCL5; *E*, CCL3; *F*, CCL4; *G*, CCL2; *H*, CXCL10; *I*, C4b; and *J*, Lcn2. RNA preparation and qRT-PCR was performed as described in Materials and Methods. Note different scale of y-axis for the various samples (*A – J*). Values are mean ± s.e.m. (*** $P < 0.001$, ** $P < 0.01$, * $P < 0.05$; ANOVA and Fisher's PLSD post hoc test; n = 3 – 6 animals per group/genotype). See Supplemental Fig. 1 for the corresponding data obtained for Line 1 mice.
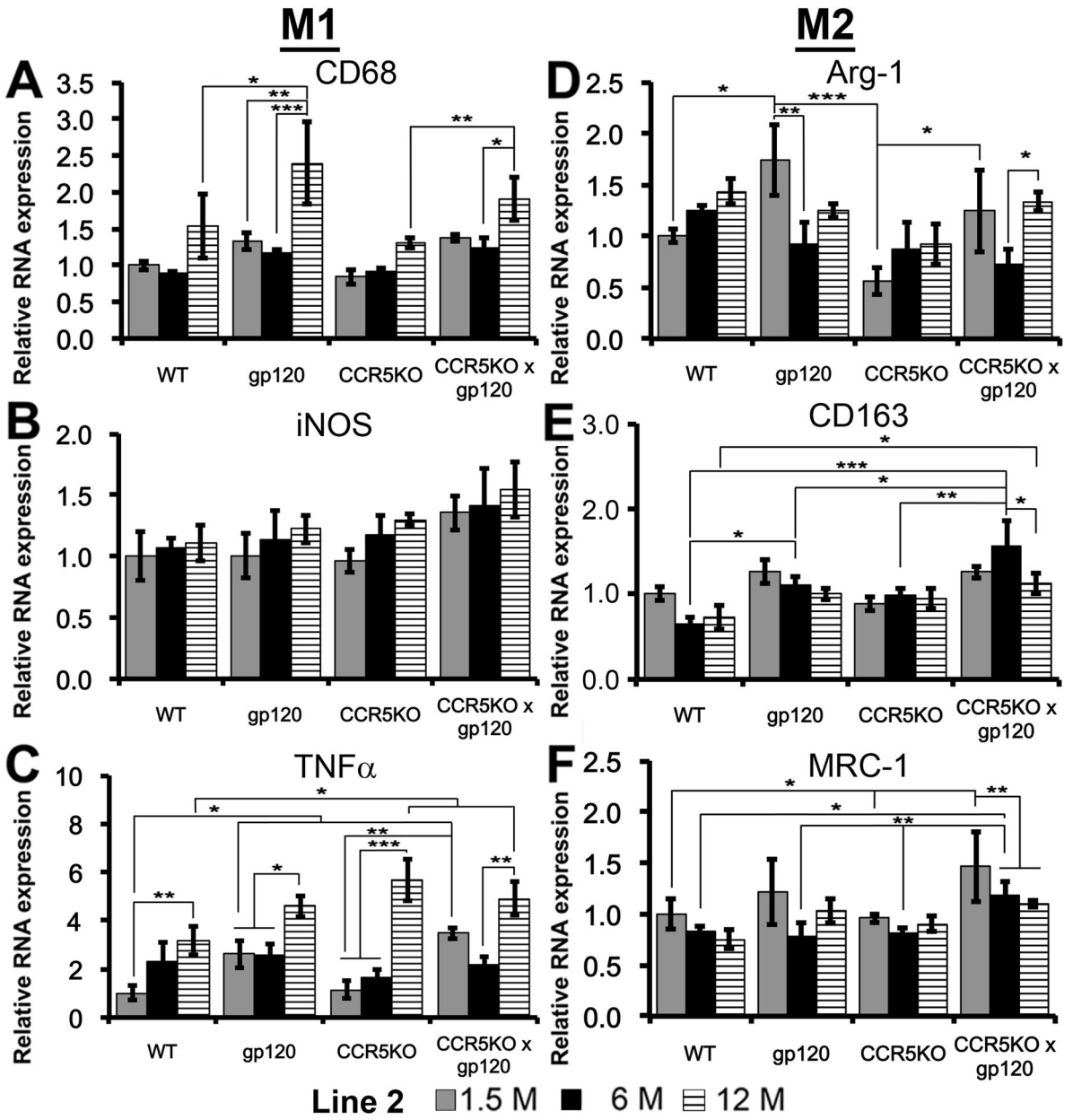
FIGURE 7.
Effect of CCR5 knockout on expression of M1 and M2-type markers of microglia and macrophages in brains of Line 2 mice: *A*, CD68; *B*, iNOS; *C*, TNFα; *D*, Arg-1; *E*, CD163; *F*, MRC-1. Preparation of RNA and qRT-PCR were performed as described in Materials and Methods. Note different scales of y-axis for the various samples (*A* – *F*). Values are mean ± s.e.m. (*** $P < 0.001$, ** $P < 0.01$, * $P < 0.05$; ANOVA and Fisher's PLSD post hoc test; n = 3 animals per group/genotype).
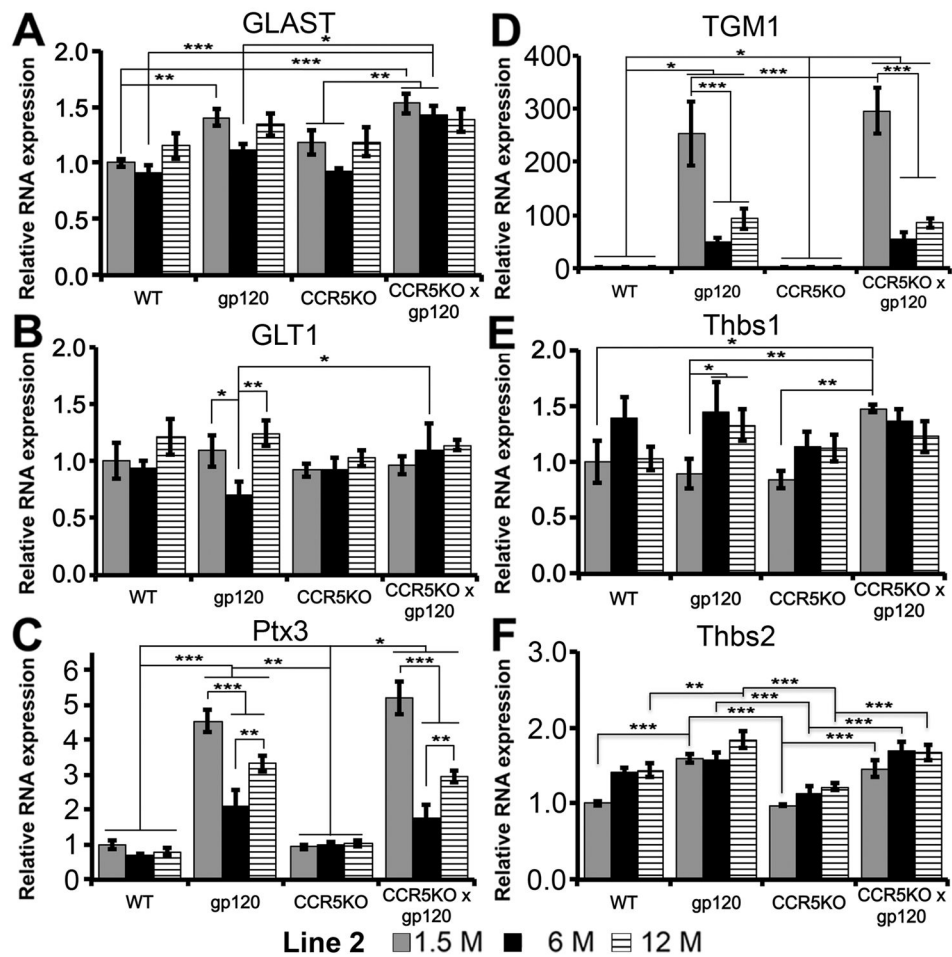
FIGURE 8.
Changes in expression of astrocyte markers in gp120tg brains in the presence and absence of CCR5. *A*, GLAST; *B*, GLT1; *C*, Ptx3; *D*, TGM1; *E*, Thbs1; *F*, Thbs2. Preparation of RNA and qRT-PCR were performed as described in Materials and Methods. Note different scales of y-axis for the various samples (*A* –*F*). Values are mean ± s.e.m. (*** $P < 0.001$, ** $P < 0.01$, * $P < 0.05$; ANOVA and Fisher's PLSD post hoc test; n = 3 animals per group/ genotype).

FIGURE 9.
Effect of CCR5-deficiency on proteins of the innate immune system and macrophages/
microglia in the CNS. Protein extracts of whole brains of Line 2 mice were prepared as
described in Materials and Methods and analyzed by ELISA (*A, C– E*). *A*, LCN2
concentrations are elevated in HIVgp120tg brains independently of CCR5 genotype at 1.5,
3, 6 and 12 months. *C*, CXCL12 (at 3, 6 and 12 months); *D*, CCL5 and, *E*, CCL2 protein at
6 months; n = 3 – 6 animals per group/genotype (*A, C– E*). LCN2 is localized in astrocytes
(*B*; overlap of GFAP with LCN2, yellow-orange, middle panel). LCN2 positive cells are
located in close proximity to some microglia (Iba1+, left panel) and neurons (MAP-2+, right
panel) in gp120tg brains. Microglial TNFα is increased in gp120tg brains in CCR5WT and
KO (*F, G*). Brain sections were stained for Iba1 and the cytokine as indicated.
Immunostaining and deconvolution microscopy was performed as described in Materials
and Methods. Threshold segmentation for Iba1 fluorescence was used to define areas

occupied by microglial cell bodies and processes. Specific TNFα fluorescence intensities were estimated in microglial cells and normalized for microglial cell number (***G***). Images show hippocampal CA1 region in brain sections of gp120tg (***B***) and WT (***F***) that were stained as indicated; scale bar 20 μm. CCR5-deficiency restricts the number of CD11b$^+$CD45^{low} cells in the brain. Cells were isolated from whole brains and spleens and analyzed by flow cytometry (***H***). Representative dot blots from analyses of one out of four independent experiments for microglial/mononuclear cells in brains (upper dot blot panels) and spleens (lower dot blot panels) of mice from line 2 with the indicated genotype. Gates indicate sub-population of CD11b$^+$CD45^{low} (resident microglia/macrophages, left gate) and CD11b$^+$CD45^{high} cells (infiltrating peripheral monocytes/macrophages, right gate). Numbers associated with gates show the respective percentage of the total cell population in the gate. In each of the experiments brain cell suspensions were pooled from five mice per genotype. Splenocytes from one representative animal per genotype are shown to demonstrate the presence of peripheral CD11b$^+$CD45^{high} cells (***H***, lower panel). Each plot represents the analysis of $4 - 10 \times 10^4$ events. Quantification of CD11b$^+$CD45^{low} cells (four independent experiments; ***I***). Values are mean ± s.e.m. (*** $P < 0.001$, ** $P < 0.01$, * $P < 0.05$; ANOVA and Fisher's PLSD post hoc test.
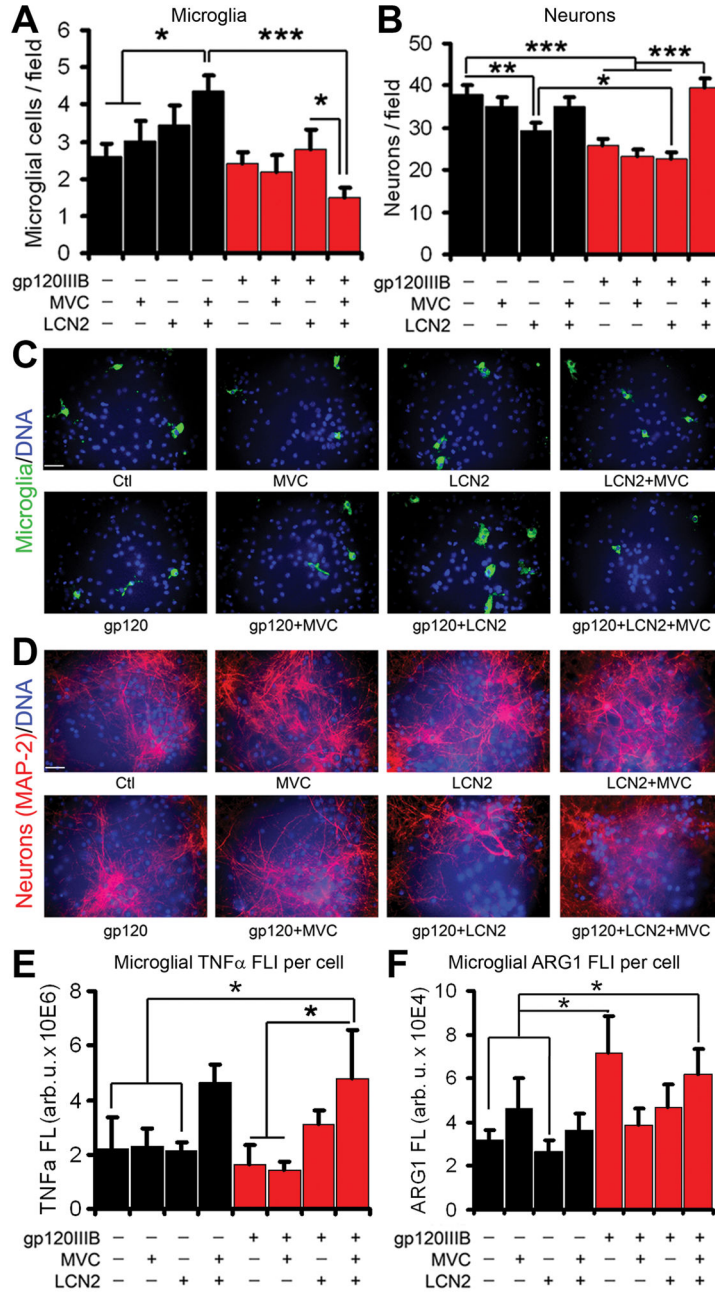
FIGURE 10.
LCN2 and interruption of CCR5 signaling reduce in combination microglial cell numbers and protect neurons in the presence of a CXCR4-using HIVgp120 from toxicity. Seventeen day old mixed neuronal-glial cerebrocortical cell cultures from Line 2 WT mouse embryos were exposed to the CXCR4-using gp120 of HIV-1$_{IIIB}$ (1 nM) in the presence or absence of LCN2 (4 nM) or the CCR5 inhibitor Maraviroc (MVC; 5 nM) for three days. Controls received vehicle only. After fixation and labeling of microglia, neurons and nuclear DNA with Tomato lectin, anti MAP-2 antibody and Hoechst33342, respectively, the cell cultures were analyzed by fluorescence microscopy (five fields each per 9 – 10 replicates per

condition). ***A***, Microglial cell numbers. ***B***, Neuronal cell numbers. Representative images of microglia (***C***) and of neurons (***D***). Scale bars, 40 μm. Microglial TNFα is increased in cerebrocortical cells exposed to LCN2 + MVC with and without gp120 (***E***) whereas ARG1 is elevated by gp120 alone and in combination with LCN2 + MVC (***F***). Cerebrocortical cell cultures grown on glass coverslips were incubated with LCN2, MVC and gp120 as described above and stained with antibody against TNFα or ARG1 and Tomato lectin to label microglia. Immunostaining and microscopy was performed as described in Materials and Methods. Threshold segmentation for Tomato lectin fluorescence was used to define areas occupied by microglial cell bodies. Specific fluorescence intensities for TNFα and ARG1 were estimated in microglia and normalized for cell number (***E, F***). Values are mean ± s.e.m. (*** $P < 0.001$, ** $P < 0.01$, * $P < 0.05$; ANOVA and Fisher's PLSD post hoc test; an average of 4,845 cells was counted (***A, B***) and an average of 226 cells analyzed (***E, F***) per condition in two independent experiments each for (***A – D***) and (***E, F***).

Table I

Primers for qRT-PCR

Gene/Target	GenBank	Primer Name	Primer Sequence (5'-3')	bp	Product size (bp)
Arg-1	NM_007482.3	mARG-1_Jang_Fwd**	CGCCTTTCTCAAAAGGACAG	19	204
		mARG-1_Jang_Rev**	CCAGCTCTTCATTGGCTTTC	20	
C4b / C4	NM_009780.2	C4b-a forward	AGACCCACGGGCTACACTT	19	220
		C4b-a reverse	GCATCCCATGCGTATTCCACA	21	
Ccl2 / Mcp1	NM_011333.3	mCcl2 Fwd	CCCAATGAGTAGGCTGGAGA	20	125
		mCcl2 Rev	TCTGGACCCATTCCTTCTTG	20	
Ccl3 / Mip1a	NM_011337.2	mCcl3 F-3	GCGCCATATGGAGCTGACA	19	72
		mCcl3 R-3	GATGAATTGGCGTGGAATCTTC	22	
Ccl4 / Mip1b	NM_013652.2	mCcl4 F-3	AGGGTTCTCAGCACCAATGG	20	69
		mCcl4 R-3	AGCTGCCGGGAGGTGTAAG	19	
Ccl5 / RANTES	NM_013653.3	mCcl5 Fwd2	ACACCACTCCCTGCTGCTTT	20	81
		mCcl5 Rev2	TGCTGCTGGTGTAGAAATACTCCTT	25	
CCR5 / CD195	NM_009917.5	mCCR5 F-3	CGAAAACACATGGTCAAACG	20	100
		mCCR5 R-3	GTTCTCCTGTGGATCGGGTA	20	
CD68	NM_009853.1	mCD68_Fwd***	CCACAGGCAGCACAGTGGACA	21	87
		mCD68_Rev***	TCCACAGCAGAAGCTTTGGCCC	22	
CD163	NM_001170395.1	mCD163_Fwd****	CCTCCTCATTGTCTTCCTCCTGTG	24	158
		mCD163_Rev****	CATCCGCCTTTGAATCCATCTCTTG	25	
CXCL10	NM_021274.2	mCXCL10frw*	GCCGTCATTTTCTGCCTCAT	20	101
		mCXCL10rev*	GGCCCGTCATCGATATGG	18	
CXCR4 / CD184	NM_009911.3	mCXCR4 F-3	CTGGCTGAAAAGGCAGTCTATGT	23	79
		mCXCR4 R-3	CGTCGGCAAAGATGAAGTCA	20	
GAPDH	NM_008084.2	mGAPDH forward	AGGTCGGTGTGAACGGATTTG	21	123
		mGAPDH reverse	TGTAGACCATGTAGTTGAGGTCA	23	
gp120-HIV-1	M19921	vHIVgp120 Fwd	TGAGCCAATTCCCATACATTATTG	24	81

Gene/Target	GenBank	Primer Name	Primer Sequence (5'-3')	bp	Product size (bp)
		vHIVgp120 Rev	CCTGTTCCATTGAACGTCTTATTATTAC	28	
Glt1/Slc1a2	NM_001077515.2	mGlt1/Slc1a2_Fwd	GGTGTATTACATGTCCACGACCAT	24	109
		mGlt1/Slc1a2_Rev	CTTCCCGGGCCCTAGCT	17	
Glast/Slc1a3	NM_148938.3	mGlast/Slc1a3_Fwd2	TCCGCCGCTCGCTAAG	16	61
		mGlast/Slc1a3_Rev2	GGCTACGTGGAGGTGAATTCC	21	
iNOS	NM_010927.3	mINOS_Crain_Fwd *****	TGACGCTCGGAACTGTAGCAC	21	98
		mINOS_Crain_Rev *****	TGATGGCCGACCTGATGTT	19	
Lcn2 / NGAL	NM_008491.1	mLcn2 Fwd2	GCCCCATCTCTGCTCACTGT	20	105
		mLcn2 Rev2	TTTTTCTGGACCGCATTGC	20	
Mrc1	NM_008625.2	mMRC-1_Jang_Fwd **	TGGCTACCAGGAAGTCCATC	20	217
		mMRC-1_Jang_Rev **	TGTAGCAGTGGCCTGCATAG	20	
Ptx3	NM_008987.3	mPtx3_Fwd2	GCTCATGCTTTGGAGCGTTT	20	61
		mPtx3_Rev2	GCCGGGAGAGATAGTGTGA	20	
SDF-1/CXCL12	NM_001012477.2	mSDF1 F-1	TGCCCCTGCCGGTTCT	16	70
		mSDF1 R-1	GAGTGTTGAGGATTTTCAGATGCTT	25	
Thbs1	NM_011580.3	mThbs1 Fwd3	TGCCATGGCCAACAAACA	18	100
		mThbs1 Rev3	GTAGTGACCCAGGTAGTTGCACTTAG	26	
Thbs2	NM_011581.3	mThbs2 Fwd3	AATTCGTCACCAAGGCAAAGA	21	81
		mThbs2 Rev3	GACCCAAACTCGTCGAAACC	20	
TNFα	NM_013693.2	mTNF-a_Jang_Fwd2 **	CATCTTCTCAAAATTCGAGTGACAA	25	411
		mTNF-a_Jang_Rev2 **	ACTTGGGCAGATTGACCTCAG	21	
Tgm	NM_001161715.1	mTgm1_Fwd	TCTGGGCTCGTTGTTGTGG	19	194
		mTgm1_Rev	AACCAGCATTCCCTCTCGGAT	21	

* Khorooshi, R. & Owens, T. Injury-induced type I IFN signaling regulates inflammatory responses in the central nervous system. J Immunol 185, 1258–1264, doi:jimmunol.0901753 [pii] 10.4049/jimmunol.0901753 (2010).

** Jang E, Lee S, Kim JH, Kim JH, Seo JW, et al. 2013. Secreted protein lipocalin-2 promotes microglial M1 polarization. FASEB J 27: 1176–90

*** Kobayashi K, Imagama S, Ohgomori T, Hirano K, Uchimura K, et al. 2013. Minocycline selectively inhibits M1 polarization of microglia. Cell Death Dis 4: e525

***** 2010Ly LV, Baghat A, Versluis M, Jordanova ES, Luyten GP, et al. 2010. In aged mice, outgrowth of intraocular melanoma depends on proangiogenic M2-type macrophages. J Immunol 185: 3481–8

***** Crain JM, Nikodemova M, Watters JJ. 2013. Microglia express distinct M1 and M2 phenotypic markers in the postnatal and adult central nervous system in male and female mice. J Neurosci Res 91: 1143–51

Table II

Comparison of Differential CNS Gene Expression in HIV Patients and HIVgp120tg Mice

No. of Overlapping CNS-Expressed Genes (*P*-Value)	Human CNS Specimen (NNTC)[*]								
	Frontal cortex			Neostriatum			White Matter		
CCR5KO x HIVgp120tg mice	HIVE/NCI 784 genes**	HIV/NCI 6 genes**	HIV No NCI 4 genes**	HIVE/NCI 593 genes**	HIV/NCI 62 genes**	HIV No NCI 72 genes**	HIVE/NCI 76 genes**	HIV/NCI 6 genes**	HIV/No NCI 5 genes**
CCR5WT-specific 734 genes	32 (0.345)	0	0	39 (2.79×10^{-4})	1 (0.85)	3 (0.49)	3 (0.37)	0	0
CCR5WT/KO-common 461 genes	30 (0.007)	0	0	83 ($< 1 \times 10^{-23}$)	7 (2.0×10^{-4})	4 (0.087)	15 (4.39×10^{-10})	0	0
CCR5KO-specific 1305 genes	87 (3.1×10^{-6})	1 (0.39)	0	64 (4.18×10^{-5})	3 (0.66)	6 (0.336)	17 (2.8×10^{-7})	0	0

[*] NNTC, National NeuroAIDS Tissue Consortium. The specimen are described in detail in Gelman BB, Chen T, Lisinicchia JG, Soukup VM, Carnical JR, et al. (2012) The National NeuroAIDS Tissue Consortium Brain Gene Array: Two Types of HIV-Associated Neurocognitive Impairment. PLoS ONE 7(9): e46178. doi:10.1371/journal.pone.0046178

[**] The numbers refer to genes mapped by Ingenuity Pathway Analysis (Ingenuity® Systems). Some genes were represented by more than one gene probe.

Comparisons were performed using Biomart and Genespring softwares as mentioned under Methods.

HIVE, HIV encephalitis; NCI, neurocognitive impairment; all gene numbers are versus HIV-negative control.

Table III

Canonical pathways affected by differential gene expression

	P-value:	Molecules in CP[*]	Ratio
CCR5WT-Specific Genes			
A): Role of Macrophages, Fibroblasts and Endothelial Cells in Rheumatoid Arthritis	1.87E-03	20/290	0.07
B): Pathogenesis of Multiple Sclerosis	2.16E-03	3/9	0.33
C): Cytotoxic T Lymphocyte-mediated Apoptosis of Target Cells	3.82E-03	6/54	0.11
D): NF-kB Activation by Viruses	4.15E-03	8/73	0.11
E): CCR5 Signaling in Macrophages	5.57E-03	7/67	0.10
CCR5WT & KO Common Genes			
F): Communication between Innate and Adaptive Immune Cells	2.90E-07	11/82	0.13
G): Hepatic Fibrosis / Hepatic Stellate Cell Activation	2.66E-06	14/132	0.11
H): Interferon Signaling	4.60E-06	7/31	0.23
I): Type I Diabetes Mellitus Signaling	4.75E-06	12/104	0.12
J): TREM1 Signaling	5.33E-06	9/58	0.16
CCR5KO-Specific Genes			
K): GABA Receptor Signaling	4.37E-04	10/47	0.21
L): LPS/IL-1 Mediated Inhibition of RXR Function	5.83E-03	22/196	0.11
M): Mineralocorticoid Biosynthesis	8.56E-03	3/7	0.43
N): Huntington's Disease Signaling	9.28E-03	23/216	0.11
O): Clathrin-mediated Endocytosis Signaling	1.29E-02	19/172	0.11

Note that the positions A–O on this table correspond to panels A–O in Fig. 4.

[*] CP, canonical pathway.